KINETIC AND THERMODYNAMIC ASPECTS OF REACTIONS INVOLVING THIYL RADICALS: A COMPUTATIONAL APPROACH

by

Volkan Fındık

B.S., Integrated B.S. and M.S. Program in Teaching Chemistry, Boğaziçi University, 2015

Submitted to the Institute for Graduate Studies in
Science and Engineering in partial fulfillment of
the requirements for the degree of
Master of Science

Graduate Program in Chemistry
Boğaziçi University
2018

To My Family

ACKNOWLEDGEMENTS

I would like to express my sincere gratitude to my thesis advisors Prof. Viktorya Aviyente and Assoc. Prof. Şaron Çatak for their support, patience and guidance.

My hearty thanks go to all current and former members of Computational Chemistry and Biochemistry group (CCBG) for their friendship and support.

I would like to thank to my best friends Hakan Arpacı and Salim Oğur for their marvelous support.

Finally, I would like to express my deepest gratitude to my mother and father for their continuous love and support throughout my life.

ABSTRACT

KINETIC AND THERMODYNAMIC ASPECTS OF REACTIONS INVOLVING THIYL RADICALS: A COMPUTATIONAL APPROACH

In this study, the kinetics of the addition of different phenylthio radicals on the thiol-ene reactions mechanism have been computationally investigated for the first time. The contributions of substituents are examined by Density Functional Theory (DFT) calculations. It is known that the reaction mechanism of thiol-ene reactions depends upon the k_P/k_{CT} ratio, where k_P is the rate constant of phenylthio radical addition to unsaturated alkene and k_{CT} is the rate constant of hydrogen abstraction of newly formed carbon centered radical from the thiol. The M06-2X/6-31++G(d,p) level of theory is used to carry out geometry optimizations and energetics of eleven reactions. The activation energy barrier of the addition reaction is strongly controlled by the electrophilic character of phenylthio radicals and the singlet-triplet gap (S-T gap) of the alkenes. For this reason, the functional groups on the alkene and phenylthio radical have an importance in order to understand the reaction kinetics of the propagation step. It is shown that the transition state structure is responsible for the lower activation energy barrier of the chain transfer step due to the stabilization effect of intramolecular interactions. Our study has shown that the substituents on the thiol as well as the substituents on the alkene have an important effect on the kp/kct ratio as well as the substituents on the alkene. The computational method described in this study can be applied in the synthesis of the desired polymers by modifying the substituents.

In addition to the investigation of thiol-ene reaction energetics and kinetics, the solvent effect on the hydrogen abstraction reaction of alkyl radical from thiol is examined by implicit solvent model. Water and acetonitrile are chosen as solvents to show the effect of the polarity of solvent. For this purpose, three different reactions are modeled at the M06-2X/6-31++G(d,p) level of theory. The results showed that the role of solvent on the thiol-alkyl reactions can be predicted by methodology used in this thesis.

ÖZET

TİYİL RADİKALİ İÇEREN REAKSİYONLARIN TERMODİNAMİK VE KİNETİK ÖZELLİKLERİNE HESAPSAL BİR YAKLAŞIM

Bu çalışmada, ilk defa olarak sübstitüentler eklenmiş feniltiyo radikallerinin tiyol-alken tepkime mekanizması üzerindeki etkisi hesapsal olarak incelenmiştir. Sübstitüentlerin etkisi Yoğunluk Fonksiyonları Teorisi (DFT) ile incelenmiştir. Daha önce bilinen sonuçlar göz önüne alındığında, tiyol-alken tepkimelerinin reaksiyon mekanizmasının k_P/k_{CT} oranına bağlı olduğu görülmektedir, k_P feniltiyo radikalinin alkene olan katılma tepkimesinin hız sabitini gösterirken k_{CT} yeni oluşan karbon radikalinin tiyollerden hidrojen koparma reaksiyonun hız sabitini göstermektedir. Bütün geometri optimizasyonları ve enerji hesaplamaları M06-2X/6-31++G(d,p) yöntemleriyle gerçekleştirilmiştir. Polimerizasyonun yayılma ayağının aktivasyon enerjisi feniltiyo radikalin elektrofil karakterine ve alkenin singlet-triplet aralığı (S-T Gap) tarafından kontrol edilmektedir. Belirtilen nedenlerden dolayı tiyol radikalinin ve alkenin üzerindeki fonksiyonel gruplar yayılma tepkimesinin kinetiğini anlamada büyük öneme sahiptirler. Zincir transfer adımının düşük aktivasyon enerji bariyerine sahip olması geçiş konumundaki moleküler yapıdan kaynaklı molekül içi enerji stabilizasyonunu sağlayan etkileşimlerin olması sebep olmuştur. Bu çalışma alkenin üzerindeki sübstitüentlerin k_P/k_{CT} oranın üzerindeki etkisi kadar tiyollerin üzerindeki sübstitüenlerin etkisi olduğunu göstermiştir. Ayrıca, bu çalışmada belirtilen hesapsal yöntemler yardımıyla istenilen polimerler sübstitüentler değiştirilerek çeşitlendirilebilirler.

Tiyol-alken reaksiyonlarının enerji ve kinetiğine ek olarak, alkil radikallerinin tiyollerden hidrojen koparma tepkimeleri çözücü modelleriyle çalışılmıştır. Polar çözücünün etkisini göstermek amacıyla çalışmalarda su ve asetonitril kullanılmıştır. Bu amaç doğrultusunda üç farklı tepkime M06-2X/6-31++G(d,p) seviyesinde modellenmiştir.

TABLE OF CONTENTS

LIST OF FIGURES

LIST OF TABLES

LIST OF SYMBOLS

$E^{‡}$	Electronic activation energy
E_c^{VWN}	Vosko-Wilk-Nusair correlation functional
E_x^{exact}	Exact exchange energy
$E_c[\rho]$	Correlation energy
$E_x[\rho]$	Exchange energy
$E_{\sigma\sigma^*}$	Non-covalent contributions to the energy
$G^{‡}$	Gibbs free energy of activation
$J[\rho]$	Coulomb energy
$T[\rho]$	Kinetic energy of interacting electrons
$T_s[\rho]$	Kinetic energy of non-interacting electrons
U_x^{σ}	Exchange energy density
$V_{ee}[\rho(\mathbf{r})]$	Interelectronic interactions
$V_{ext}(\mathbf{r})$	External potential
V_{KS}	Kohn-Sham potential
$\Delta G^{‡}_{CT}$	Gibbs free energy of activation barrier of chain transfer reaction
$\Delta G^{‡}_{P}$	Gibbs free energy of activation barrier of propagation reaction
ΔG^{o}_{CT}	Gibbs free energy of chain transfer reaction
ΔG^{o}_{P}	Gibbs free energy of propagation reaction
ΔE_x^{B88}	Becke's gradient correction
ΔE_0	Relative electronic energy at 0 K
ΔE_{0+ZPE}	Sum of the change in electronic energy and zero point energy at 0 K
$\Delta H^{‡}_{CT}$	Enthalpy of activation barrier of chain transfer reaction
$\Delta H^{‡}_{P}$	Enthalpy of activation barrier of propagation reaction
ΔH^{o}_{CT}	Enthalpy of chain transfer reaction
ΔH^{o}_{P}	Enthalpy of propagation reaction
ΔH_{rxn}	Enthalpy of overall reaction
$v(r)$	External potential
$\rho(r)$	Electron density
ψ_i	Kohn-Sham orbital

LIST OF ACRONYMS/ABBREVIATIONS

B3LYP	Becke-3-parameter Lee-Yang-Parr functional
B88	Becke 88 Exchange Functional
DFT	Density Functional Theory
GGA	Generalized Gradient Approximation
$\hat{H}$	Hamiltonian operator
h_i	One-electron hamiltonian
HF	Hartree-Fock
J	Charge Transfer Integral
K	Exchange Integral
KS	Kohn-Sham
M06-2X	Minnesota functional with 54% HF exchange
RSE_{std}	Standard Radical Stabilization Energy
RSE_z	Zavitsas's Inherent Radical Stabilization method
S-T Gap	Singlet-Triplet Gap
SOMO	Singly Occupied Molecular Orbital

1. INTRODUCTION

The improvements of high quality materials are necessary to meet demands of industrial applications. Tailor-made type molecular structures considerably fulfill such requirements in terms of designing materials with the control over construction, functionality and especially physico-chemical characteristics.

The click reactions have gained importance after Sharpless identified their properties in 2001 [1]. There are many advantageous click reactions in chemical synthesis and they can be listed as: giving high yield without byproduct or easily removable byproduct with the non-chromatographic method, having short reaction times, having substituent and solvent tolerance, insensitivity towards water and oxygen. Even if there are series of reactions which are known as 'click' reactions, research has been mainly carried out by on the Cu(I)-mediated Huisgen reaction between an alkyne and an azide due to the ease of application, effortless reaction conditions and orthogonality [2-4]. However, the immense advantages of Cu(I)-mediated alkyne-azide reaction gave an opportunity and encouragement to researchers to investigate other type of reactions which have click properties. For this reason, the application areas of click reactions are now numerous, nucleophilic ring-opening of strained heterocyclic electrophiles, Diels-Alder reactions and photo initiated thiol-ene reactions which are based upon the hydrothiolation of alkenes can be pointed as the mostly preferred ones.

The reactions between thiols and alkenes are not a recent exploration, the affinity of sulfur radical to unsaturated alkenes is known for more than 100 years [5]. Even if the thiol-ene reactions can be initiated thermally, initiation efficiency with UV is higher, and that gives an opportunity to initiate reaction by sunlight. The reaction mechanism of thiol-ene reactions can be basically described as: sulfur radical addition to unsaturated alkene with the anti-Markovnikov rule and hydrogen abstraction of carbon centered radical from the thiol as shown in Figure 1.1.

Initial usage of thiol-ene reactions is in the area of polymer synthesis with excellent network was demonstrated in the work of Hoyle and Bowman [6-18]. In last decade, due to

the promising and facile properties of thiol-ene reactions, a field of applications has been developed far beyond the polymer synthesis. The areas including thiol-ene reactions are expanded to dendrimer, hydrogel synthesis [19,20], surface patterning [21], drug delivery systems [22], electrooptical materials [23].

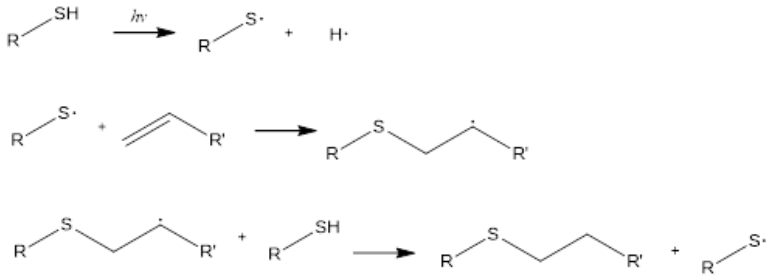

Figure 1.1. Thiol-Ene Click Reaction.

The photoinitiated thiol-ene click reactions have basically three steps. These steps can be expressed as initiation, propagation and chain transfer as shown in Figure 1.2. In the initiation step, a thiyl radical is formed after the thiol is exposed to UV radiation. After that, the thiyl radical attacks to the unactivated alkene by obeying the Anti-Markovnikov rule and a new carbon centered radical intermediate is formed in the propagation step. After the propagation step, the radical intermediate has two possibilities, one of them is to abstract a hydrogen from thiol, the other is the attack to an alkene yielding the homopolymerization. The pathway is controlled by the relative rates of chain transfer and chain growth steps that both depend upon the characteristics of the alkene and the carbon centered radical intermediate [10].

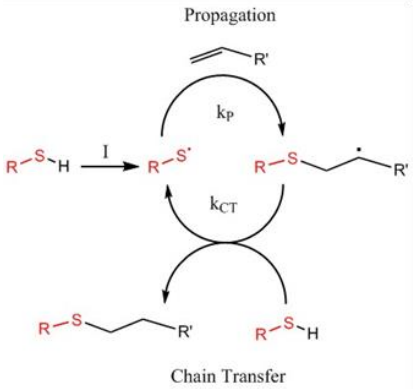

Figure 1.2. Propagation and chain transfer steps of thiol-ene click chemistry [16].

Even if some studies [12,14,18,24] claim that the reaction mechanism of thiol-ene reaction is primarily controlled by the functionality of the alkene, in the experimental studies [10,25,26,27] the overall reaction kinetics are seen to depend on the alkenes and the thiols. Notwithstanding there are many application fields of thiol-ene reactions, the studies about the kinetic investigation of reaction mechanism is highly limited. For this reason, the determination of factors that influence the structure-reactivity relationship gain importance in understanding the origin of the thiol-ene reactivity.

It is reported by Bowman and co-workers that the ratio of the rate of propagation to rate of chain transfer (k_P/k_{CT}) is crucial to manage the overall reaction kinetics. The dependency of kinetic parameter and reaction order of thiol-ene reaction is displayed in Figure 1.3. Despite the fact that k_P/k_{CT} gives a reasonable understanding about the reaction mechanism, reaction and activation enthalpies, free energy activation barriers, k_P and k_{CT} individual parameters are extremely important for thiol-ene reactions [24]. In addition to the energetics of thiol-ene reactions, polar effects [28], non-polar effects [29], intermolecular forces [30] are essential for radicalic reactions to figure out the reaction kinetics.

$$\text{if} \quad \begin{cases} k_P/k_{CT} \gg 1 & \\ k_P/k_{CT} \sim 1 & \text{overall rate depends on} \quad [SH]^{1/2}\,[C{=}C]^{1/2} \\ k_P/k_{CT} \ll 1 & [C{=}C]^{1} \end{cases}$$

Figure 1.3. Relationship between k_P/k_{CT} and concentration.

The addition reaction between the thiyl radical and the alkene is highly fast and often reversible [31]. Besides, the exothermicity is relatively high, reaction enthalpy of thiol addition to electron rich vinyl ether double bond is around -10.5 kcal mol^{-1} and -22.6 kcal mol^{-1} for the electron deficient N-alkyl maleimide [32]. For this reason, the addition rate of electron efficient alkenes is more rapid than the poor ones for the same thiol [8,33]. The stability of the carbon centered radical intermediate has an importance on the regioselectivity of thiyl radical addition to alkenes [34]. Despite the fact that thiol-ene

reactions have high regioselectivity, thiyl radical addition to linear alkenes shows low stereoselectivity. In the cyclic and the substituted cyclohexene case, stereoselectivity is highly possible because of the steric hindrance [35].

In this study, the propagation and the chain transfer steps of thiol-ene reactions with different types of thiols and alkenes are investigated. Although the effect of alkene functionality on the thiol-ene reactions has been studied, the effect of thiol functionality has not been studied in detail yet. The propagation rate constant k_P is affected by the alkene functionality, the type of thiyl radical and the stability of thiyl radical. The chain transfer rate constant k_P is mostly controlled by the stability of carbon centered radical. In this study, the mechanism of eleven thiol-ene reaction has been studied by using Density Functional Theory. In order to define the effects of thiol on the thiol-ene reaction, 4 different meta substituted phenylthiol radicals are chosen with the six well known and industrially used alkenes as shown Figure 1.4.

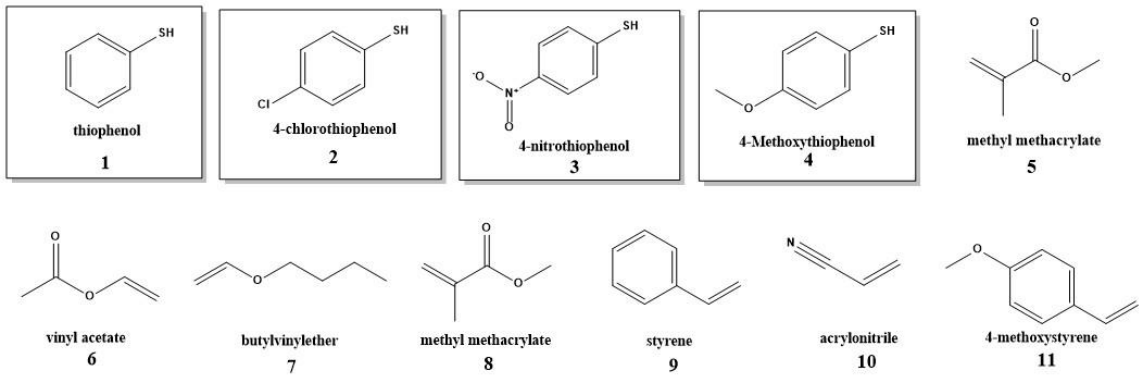

Figure 1.4. Chemical structures of thiophenols and alkenes.

In contrast to the general opinion, radicals are responsive to polar solvents [36]. For instance, protic hydrogen atom donors like phenols are less reactive in terms of hydrogen atom transfer in polar media because of the their hydrogen bonding ability [37]. Thiols are less sensitive to hydrogen bonding due to fact that they are weak hydrogen bond donors [38]. In contrast to that, it has been shown that polar solvents especially water increase the rate of hydrogen atom transfer to alkyl radical. The rate constant of hydrogen abstraction by tertiary alkyl radical is increased in water when compared to dichloromethane for the identical reaction [39]. In addition to this, the reaction between thiol and alkyl radical, the

polar transition state is stabilized by the polar solvents by leading to a decrease in activation barrier [39]. In this work, three different hydrogen abstraction reactions between thiol and alkyl radical will be studied computationally both in implicit and explicit water solution models in order to identify the effect of polar solvent on the rate constant and reaction energetics. Therefore, four different carbon centered radicals and three different thiols are selected to investigate the effect of water on the reaction as shown in Figure 1.5.

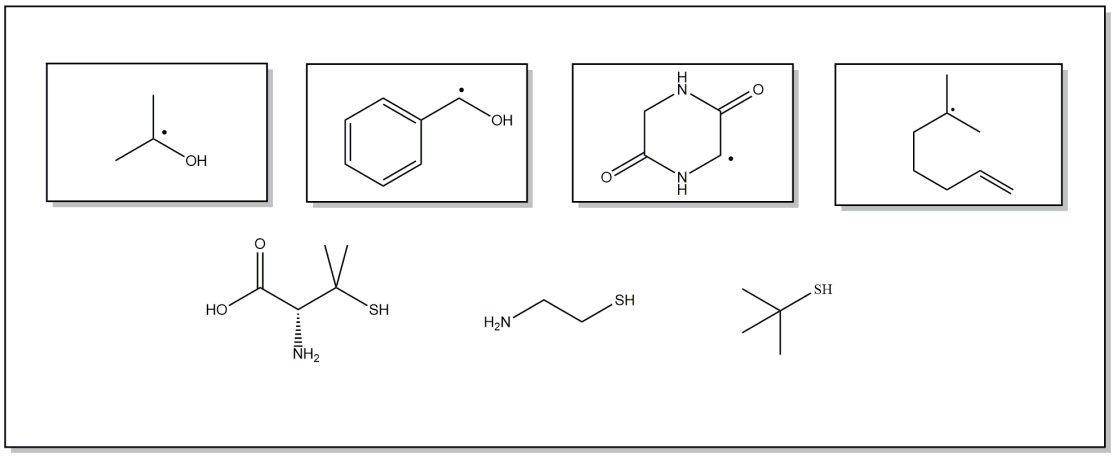

Figure 1.5. Chemical structures of alkyl radicals and thiols used to monitor the hydrogen abstraction from thiols.

2. METHODOLOGY

2.1. Density Functional Theory

Density Functional Theory (DFT) [40] is a quantum mechanical approach, which allows to calculate the electronic structure of molecules based upon a theory proposed by Kohn-Hohenberg [41,42]. Kohn-Hohenberg theorem states their ground state density is sufficient to determine the wavefunction.

The first theorem of the theory states that electron density $\rho(\mathbf{r})$ determines the external potential $V_{ext}(\mathbf{r})$ i. e. the potential due to the nuclei and the second theorem introduces the variational principle. As a result, the electron density can be computed variationally and the wavefunction, energy, position of nuclei and other related problems can be calculated [40,43].

The electron density is defined as:

$$\rho(x) = N \int \cdots \int |\Psi(x_1, x_2, \cdots, x_n)|^2 dx_1 dx_2 \cdots dx_n \tag{2.1}$$

where x represents both spin and spatial coordinates of electrons.

The electronic energy can be expressed as a functional of the electron density:

$$E[\rho] = \int v(r)\rho(r)dr + T[\rho] + V_{ee}[\rho] \tag{2.2}$$

where $T[\rho]$ is the kinetic energy of the interacting electrons and $V_{ee}[\rho]$ is the interelectronic interaction energy. The electronic energy may be rewritten as

$$E[\rho] = \int v(r)\rho(r)dr + T_s[\rho] + J[\rho] + E_{xc}[\rho] \tag{2.3}$$

with $J[\rho]$ being the coulomb energy, $T_s[\rho]$ being the kinetic energy of the non-interacting electrons and $E_{xc}[\rho]$ being the exchange-correlation energy functional. The exchange-

correlation functional is expressed as the sum of an exchange functional $E_x[\rho]$ and a correlation functional $E_c[\rho]$, although it contains also a kinetic energy term arising from the kinetic energy difference between the interacting and non-interacting electron systems. The kinetic energy term, being the measure of the freedom, and exchange-correlation energy, describing the change of opposite spin electrons (defining extra freedom to an electron), are the favorable energy contributions. The Coulomb energy term describes the unfavorable electron-electron repulsion energy and therefore disfavors the total electronic energy [44].

In Kohn-Sham density functional theory, a reference system of independent non-interacting electrons in a common, one-body potential V_{KS} yielding the same density as the real fully-interacting system is considered. More specifically, a set of independent reference orbitals ψ_i satisfying the following particle independent Schrödinger equation are imagined.

$$\left[-\frac{1}{2}\nabla^2 + V_{KS}\right]\psi_i = \varepsilon_i\psi_i \tag{2.15}$$

with the one-body potential V_{KS} defined as

$$V_{KS} = v(r) + \frac{\partial J[\rho]}{\partial \rho(r)} + \frac{\partial E_{xc}[\rho]}{\partial \rho(r)} \tag{2.16}$$

$$V_{KS} = v(r) + \frac{\rho(r')}{|r - r'|}dr' + v_{xc}(r) \tag{2.17}$$

where $v_{xc}(r)$ is the exchange-correlation potential. The independent orbitals ψ_i are known as Kohn-Sham orbitals and give the exact density by

$$\rho(r) = \sum_i^N |\psi_i|^2 \tag{2.18}$$

if the exact form of the exchange-correlation functional is known. However, the exact form of this functional is not known and approximate forms are developed starting with the local

density approximation (LDA). This approximation gives the energy of a uniform electron gas, i. e. a large number of electrons uniformly spread out in a cube accompanied with a uniform distribution of the positive charge to make the system neutral. The energy expression is

$$E[\rho] = T_s[\rho] + \int \rho(r) v(r) dr + J[\rho] + E_{xc}[\rho] + E_b \tag{2.19}$$

where E_b is the electrostatic energy of the positive background. Since the positive charge density is the negative of the electron density due to uniform distribution of particles, the energy expression is reduced to

$$E[\rho] = T_s[\rho] + E_{xc}[\rho] \tag{2.20}$$

$$E[\rho] = T_s[\rho] + E_x[\rho] + E_c[\rho] \tag{2.21}$$

The kinetic energy functional can be written as

$$T_s[\rho] = C_F \int \rho(r)^{5/3} dr \tag{2.22}$$

where C_F is a constant equal to 2.8712. The exchange functional is given by

$$E_x[\rho] = -C_x \int \rho(r)^{4/3} dr \tag{2.23}$$

with C_x being a constant equal to 0.7386. The correlation energy, $E_c[\rho]$, for a homogeneous electron gas comes from the parametrization of the results of a set of quantum Monte Carlo calculations.

The LDA method underestimates the exchange energy by about 10 per cent and does not have the correct asymptotic behavior. The exact asymptotic behavior of the exchange energy density of any finite many-electron system is given by

$$\lim_{x\to\infty} U_x^{\sigma} = -\frac{1}{r} \tag{2.24}$$

U_x^{σ} being related to $E_x[\rho]$ by

$$E_x[\rho] = \frac{1}{2}\sum_{\sigma}\int \rho_{\sigma} U_x^{\sigma} dr \tag{2.25}$$

A gradient-corrected functional is proposed by Becke

$$E_x = E_x^{LDA} - \beta\sum_{\sigma}\int \rho_{\sigma}^{4/3} \frac{x_{\sigma}^2}{1+6\beta x_{\sigma}\sinh^{-1} x_{\sigma}} dr \tag{2.26}$$

where σ denotes the electron spin, $x_{\sigma} = \frac{|\nabla\rho_{\sigma}|}{\rho_{\sigma}^{4/3}}$ and β is an empirical constant (β=0.0042). This functional is known as Becke88 (B88) functional [42].

The adiabatic connection formula connects the non-interacting Kohn-Sham reference system (λ=0) to the fully-interacting real system (λ=1) and is given by

$$E_{xc} = \int_0^1 U_{xc}^{\lambda} d\lambda \tag{2.27}$$

where λ is the interelectronic coupling-strength parameter and U_{xc}^{λ} is the potential energy of exchange-correlation at intermediate coupling strength. The adiabatic connection formula can be approximated by

$$E_{xc} = \frac{1}{2}E_x^{exact} + \frac{1}{2}U_{xc}^{LDA} \tag{2.28}$$

since $U_{xc}^{0} = E_x^{exact}$, the exact exchange energy of the Slater determinant of the Kohn-Sham orbitals, and $U_{xc}^{1} = U_{xc}^{LDA}$ [41].

The closed shell Lee-Yang-Parr (LYP) correlation functional [45] is given by

$$E_c = -a\int \frac{1}{1+d\rho^{-1/3}}\left\{\rho + b\rho^{-2/3}\left[C_F\rho^{5/3} - 2t_w + (\frac{1}{9}t_w + \frac{1}{18}\nabla^2\rho)\right]e^{-c\rho^{-1/3}}\right\}dr \quad (2.29)$$

where

$$t_w = \frac{1}{8}\frac{|\nabla\rho(r)|^2}{\rho(r)} - \frac{1}{8}\nabla^2\rho \quad (2.30)$$

The mixing of LDA, B88, E_x^{exact} and the gradient-corrected correlation functionals to give the hybrid functionals [46] involves three parameters.

$$E_{xc} = E_{xc}^{LDA} + a_0\left(E_x^{exact} - E_x^{LDA}\right) + a_x\Delta E_x^{B88} + a_c\Delta E_c^{non-local} \quad (2.31)$$

where ΔE_x^{B88} is the Becke's gradient correction to the exchange functional. In the B3LYP functional, the gradient-correction ($\Delta E_c^{non-local}$) to the correlation functional is included in LYP. However, LYP contains also a local correlation term which must be subtracted to yield the correction term only.

$$\Delta E_c^{non-local} = E_c^{LYP} - E_c^{VWN} \quad (2.32)$$

where E_c^{VWN} is the Vosko-Wilk-Nusair correlation functional, a parametrized form of the LDA correlation energy based on Monte Carlo calculations. The empirical coefficients are a_0=0.20, a_x=0.72 and a_c=0.81 [47].

2.3. Basis Sets

Basis sets describe the wavefunctions, and are necessary to solve the Schrödinger Equation. Split valence basis sets of Pople *et al.* such as 3- 21G, 6-21G, 6-31+G and 6-311G* are the most common basis sets used. The functions are splitted, i.e. the first

number denotes the primitives in the core functions, and the numbers after the hyphen represent the number of primitives used in the valence functions. Two numbers mean valence double-ζ basis, and three numbers mean valence triple-ζ basis. One can add polarization functions, and extend the basis set, describe the system better and have more mathematical flexibility in calculations. Diffuse functions can also be added, where it is not possible for the basis set to provide enough flexibility to include an electron so far away from the core. Diffuse functions are denoted by the "+" sign to heavy atoms, second "+" sing denotes diffuse functions to hydrogen atoms. Polarization functions on non-hydrogen atoms are shown by "*", and if two asterisks "**" are present, it means that the polarization functions are also added to the light atoms, hydrogen and helium.

2.4. Continuum Solvation Models

Continuum solvation models are the most efficient way to include condensed-phase effects into quantum mechanical calculations [48]. The advantage of these models is that they decrease the number of the degrees of freedom of the system by describing them in a continuous way, usually by means of a distribution function [48,49]. In continuum solvation models, the solvent is represented as a polarizable medium characterized by its static dielectric constant ε and the solute is embedded in a cavity surrounded by this dielectric medium. The total solvation free energy is defined as

$$\Delta G_{solvation} = \Delta G_{cavity} + \Delta G_{dispersion} + \Delta G_{electrostatic} + \Delta G_{repulsion} \quad (2.45)$$

where ΔG_{cavity} is the energetic cost of placing the solute in the medium. Dispersion interactions between solvent and solute are expressed as $\Delta G_{dispersion}$ which add stabilization to solvation free energy. $\Delta G_{electrostatic}$ is the electrostatic component of the solute-solvent interaction energy. $\Delta G_{repulsion}$ is the exchange solute-solvent interactons not included in the cavitation energy.

The central problem of continuum solvent models is the electrostatic problem described by the general Poisson equation:

$$-\vec{\nabla}\left[\varepsilon(\vec{r})\nabla\vec{V}(\vec{r})\right] = 4\pi\rho_M(\vec{r}) \tag{2.46}$$

simplified to

$$-\nabla^2 V(\vec{r}) = 4\pi\rho_M(\vec{r}) \text{ within } C \tag{2.47}$$

$$-\varepsilon\nabla^2 V(\vec{r}) = 0 \text{ outside } C \tag{2.48}$$

where C is the portion of space occupied by cavity, ε is dielectric function, V is the sum of electrostatic potential V_M generated by the charge distribution ρ_M and the reaction potential V_R generated by the polarization of the dielectric medium:

$$V(\vec{r}) = V_M(\vec{r}) + V_R(\vec{r}) \tag{2.49}$$

The Polarizable Continuum Model (PCM) belongs to the class of polarizable continuum solvation models [50]. In PCM, the solute is embedded in a cavity defined by a set of spheres centered on atoms (sometimes only on heavy atoms), having radii defined by the van der Waals radius of the atoms multiplied by a predefined factor (usually 1.2). The cavity surface is then subdivided into small domains (called tesserae), where the polarization charges are placed. There are three different approaches to carry out PCM calculations. The original method is called Dielectric PCM (D-PCM), the second model is the Conductor-like PCM (C-PCM) [51] in which the surrounding medium is modeled as a conductor instead of a dielectric, and the third one is an implementation whereby the PCM equations are recast in an integral equation formalism (IEF-PCM). The IEF-PCM methodology has been used in this study.

3. AIM OF THE STUDY

In the first part of this study thiol-ene reactions have been modeled, whereas in the second part of this thesis the hydrogen abstraction ability of thiyl radical in solution has been investigated.

In the propagation part of study, eleven different addition reactions are modeled to understand and determine the reasons that influence the reaction mechanisms. Methyl methacrylate, vinyl acetate, butyl vinyl ether, styrene, acrylonitrile, 4-methoxystyrene are selected because of the fact that they are mostly used alkenes in material industries. Thiophenol and its derivatives; 4-chlorothiophenol, 4-nitrothiophenol, 4-methoxythiophenols are used to understand substituent effect on sulfur radical and reaction energetics. $\Delta G^{\ddagger}_{P}$, $\Delta H^{\ddagger}_{P}$, ΔG^{o}_{P}, ΔH^{o}_{P} represent the activation barrier and reaction energies of propagation steps. Activation barriers are used to determine rate constant of each propagation reaction.

In the chain transfer, eleven reactions with the same monomers are examined to determine properties which trigger chain transfer energetics and kinetics. Among the eleven thiol-ene reaction, first five reactions are chosen with the same radical but different alkenes to eliminate the effects which result from the different types of phenylthio radical. The four of those reactions are selected to eliminate the effect of the alkene by choosing the same alkene for the reactions.

In the second part of thesis, the effects of polar solvent on the thiol-alkyl reaction energetics are investigated to identify reaction rates. For this purpose, four different thiol-alkyl reactions having experimental rate constants are selected. The experimental rate constants determined in aqueous media are benchmarked against the results of computational solvent models.

4. THIOL-ENE REACTIONS

4.1. Computational Procedure

All reactions and benchmark calculations were modeled by using the Gaussian09 software package [52]. A previous study [24] has shown that more than 4.0 kcal/mol errors are assessed at the B3LYP/6-311+G(d) level of theory for a series of thiol-ene reactions in terms of reaction enthalpies. M06-2X has been chosen because of its success in a thiol-disulfide exchange study [53]. Three different basis sets have been used to predict the best outcome in terms of reaction kinetics (6-31+G(d), 6-31++G(d,p), 6-311++G(3df,3pd)). Benchmark calculations have been carried out for five thiol-ene reactions whose experimental rate constants are known [30]. The M06-2X/6-31++G(d,p) methodology yields the best agreement with experiment (Table 4.1), therefore, all geometry optimizations, frequency, transition state and single point calculations have been performed with this methodology. Geometry optimizations are carried out in vacuum at 1.0 atm and 298.15 K. Electron affinities are determined by subtracting the electronic energies of the anions from the neutral molecules. Ionization potential energies are found by subtracting the electronic energies of the cation from the neutral molecules. Singlet state and triplet state energy differences gave the S-T gap for each alkene. Radical stabilization energies were calculated according to standard (RSE_{std})[54] equation 4.1 and Zavitsas's method (RSE_z) [55] equation 4.2. In the standard radical stabilization energy definition, bond dissociation energies $D[H-CH_3]$ and $D[H-R]$ are used to predict the stability of radical $R^{\cdot}$. In the Zavitsas's radical stability definition, bond dissociation energies $D[H_3C-CH_3]_{calc}$, $D[R-R]_{calc}$ are calculated by using Pauling's electronegativity equation [56] for the direct comparison of the different types of radical stabilities. The standard method contributes to understand the tendency of a radical to transfer hydrogen from organic molecules, while Zavitsas's model helps to understand the inherent stability of various type of radicals.

$$\mathrm{RSE_{std}(R^{\cdot})} = \mathrm{D[H-CH_3]} - \mathrm{D[H-R]} \quad (4.1)$$

$$\mathrm{RSE_z(R^{\cdot})} = 1/2(\mathrm{D[H_3C-CH_3]_{calc}} - \mathrm{D[R-R]_{calc}}) \quad (4.2)$$

$$k(T) = \kappa(T)\frac{k_B T}{h}(c^o)^{1-m}e^{(-\Delta G^{\ddagger}/RT)} \quad (4.3)$$

Rate constants are calculated by using equation 4.3 where, $k(T)$ is the reaction rate constant, R is universal gas constant (8.314 J mol^{-1} K^{-1}), $\kappa(T)$ is tunneling correction (for simplicity it is taken as 1), k_B is the Boltzmann constant (1.380658x10^{-23} J K^{-1}), T is the temperature (298.15 K), h is Planck's constant (6.6260755x10^{-34} J s), c^o is the standard unit of concentration (mol L^{-1}) (= $n/V = P^{\theta}/RT$), m is the molecularity of the reaction, and $\Delta G^{\ddagger}$is the Gibbs Free energy change between activated complex and reactants. (RS$^-$ ene$^+$) and (RS$^+$ ene$^-$) represent the polar charge transfer configurations. The energy of (RS$^-$ ene$^+$) is calculated by subtracting the electron affinity of the phenylthio radical from the ionization potential of corresponding alkene and vice versa for (RS$^+$ ene$^-$) (Table 4.2).

Table 4.1. Comparison of experimental results with calculated propagation rate constants.[1]

Substrate	6-31+G(d)	6-31++G(d,p)	6-311++G(3df,3pd)	Experimental [27]
Styrene	2.33E+07	3.54E+07	9.91E+12	2.70E+07
Methyl Methacrylate	4.48E+06	4.35E+06	7.79E+11	3.20E+06
Acrylonitrile	8.47E+04	8.37E+04	6.13E+10	4.60E+05
Butyl Vinyl Ether	2.75E+06	1.15E+05	2.33E+11	1.20E+05
Vinyl Acetate	2.98E+04	5.08E+03	1.43E+10	1.70E+04

[1] M06-2X is used as a functional for each basis set. Correlation coefficients are 0.9841, 0.9997, 0.9975, respectively. Phenylthio radical is used as radical.

Table 4.2. Calculated ionization potentials and electron affinities for alkenes and phenylthio radicals. Ionization potential, electron affinity, RS^- ene^+ and RS^+ ene^- energies are given in eV (M06-2X/6-31++G(d,p)).

Substrate	Ionization Potential	Electron Affinity	RS^- ene^+	RS^+ ene^-
Styrene	8.5	0.5	6.2	9.3
Methyl Methacrylate	10.0	0.6	7.7	9.4
Acrylonitrile	10.9	0.4	8.6	9.2
Butyl Vinyl Ether	8.7	0.8	6.4	9.6
Vinyl Acetate	9.8	0.8	7.4	9.6
Phenylthio radical	8.8	-2.3		

4.2. Benchmark Study for Thiol-Ene Reactions

Five thiol-ene reactions have been chosen for a benchmark study in order to assess the efficiency of the M06-2X/6-31++G(d,p) by comparison with the CBS-QB3 results [24] according to overall reaction (Table 4.3). The correlation between these two methods is high as seen in Figure 4.2 in terms of reaction free energies. S-H bond dissociation energy of thiophenol is around 79 kcal/mol according to the experimental result [57]. In our calculations, BDE's of thiophenols and substituted thiophenols (Table 4.4) vary between 73.67 to 78.75 kcal/mol, high correlation has been established between calculated and experimental results [58] (R^2 = 0.885) (Figure 4.2). M06-2X/6-31++G(d,p) has been chosen to investigate the energetics of thiol-ene reaction by taking into account the results of five reaction free energies and the BDE's of thiophenols.

Table 4.3. Benchmark studies for the Gibbs free energies for five thiol-ene reactions (kcal/mol) (M06-2X/6-31++G(d,p)).

			CBS-QB3	M06-2X/ 6-31++G(d,p)
Thiol	Alkene	Thioether	ΔG^{o}_{rxn}	ΔG^{o}_{rxn}
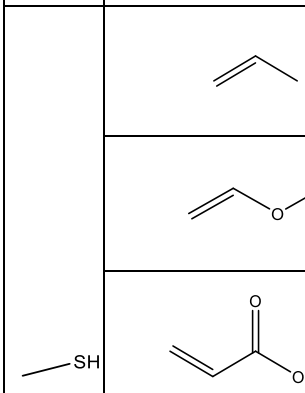			-7.7	-8.8
			-4.5	-6.0
			-8.2	-10.7
			-6.1	-6.3
			-8.3	-9.4

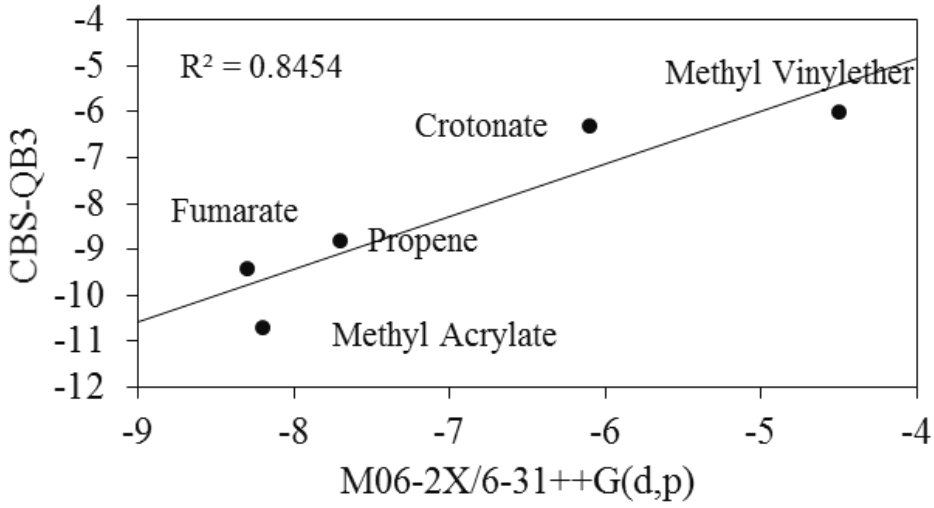

Figure 4.1. Correlation between calculated Gibbs Free energies ΔG^{o}_{rxn} (kcal/mol) of thiyl radical addition to the alkenes with two different theoretical methods.

Table 4.4. Experimental and calculated S-H bond dissociation energies (BDE) of para substituted thiophenols (kcal/mol) (M06-2X/6-31++G(d,p)).

	H, Cl, OCH_3, NO_2	Experimental [59]	M06-2X/ 6-31++G(d,p)
1	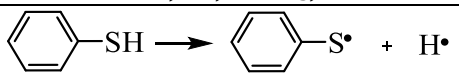	79.1	77.75
2	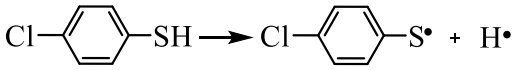	79.2	76.68
3	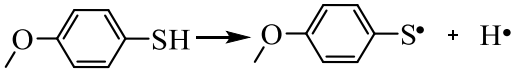	76.9	73.67
4	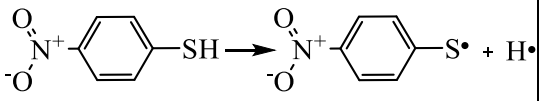	81.4	78.78

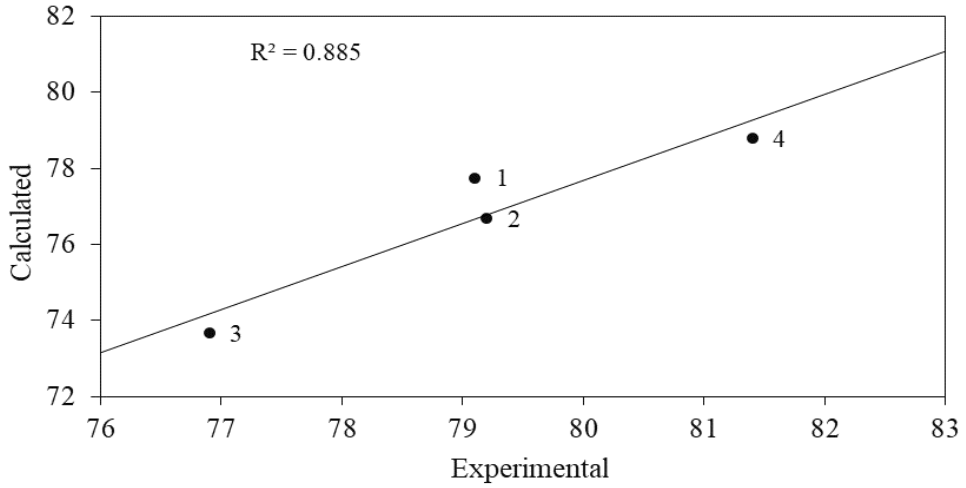

Figure 4.2. Comparison of calculated S-H BDEs of para substituted thiophenols versus experimental S-H BDEs (kcal/mol) (M06-2X/6-31++G(d,p)).

The reaction profile of the phenylthiol-ene reaction is displayed in Figure 4.3. The Gibbs free energy of activation barrier of phenylthiol radical addition to alkene is represented by $\Delta G^{\ddagger}_{P}$, the hydrogen abstraction of the carbon centered radical intermediate from phenylthiol, the chain transfer step is represented by $\Delta G^{\ddagger}_{CT}$. The reaction Gibbs free energy of propagation step, the Gibbs free energy of chain transfer and the overall reaction Gibbs free energy are expressed as $\Delta G^{o}_{P,}$ ΔG^{o}_{CT}, ΔG^{o}_{rxn}, respectively. In this thesis, the main focus will be on the propagation and chain transfer (Figure 1.2.) steps due to the fact

that the initiation step includes several photochemical and thermal initiators [60,61] according to the experimental procedure and it is not the inherent point of this study.

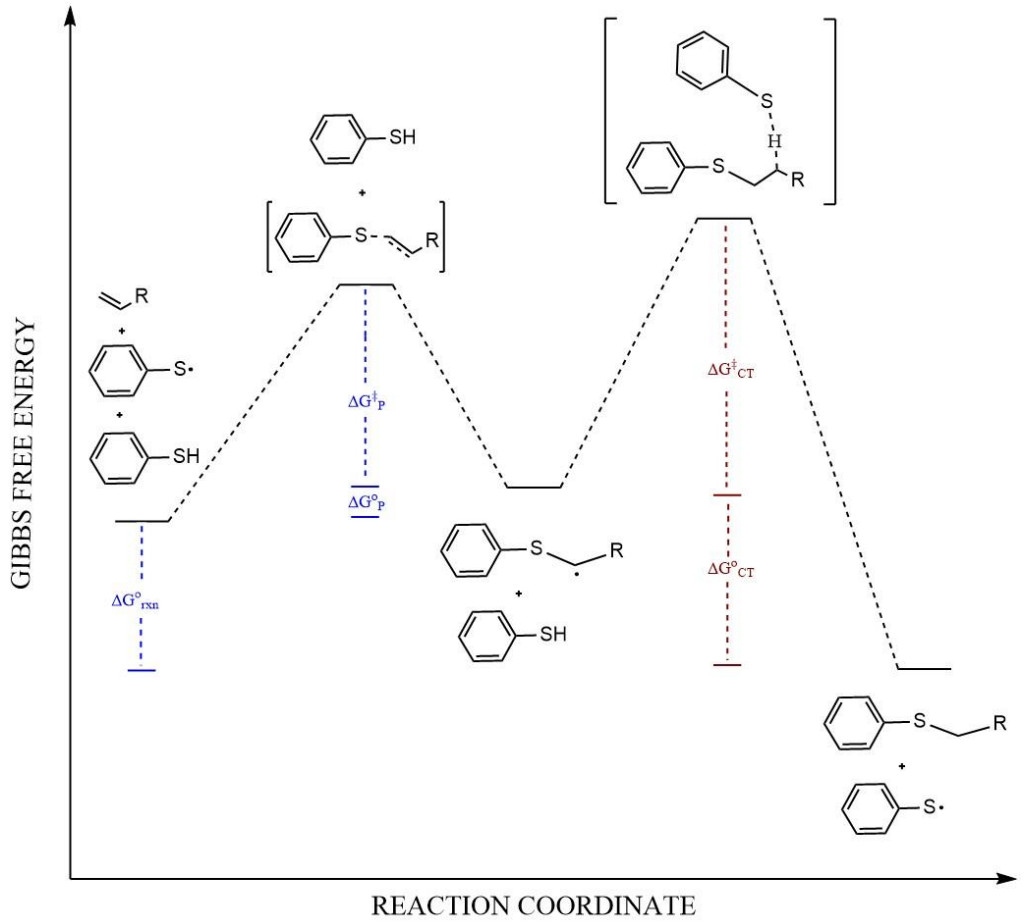

Figure 4.3. Overall reaction profile for the step-growth mechanism of radical initiated thiol−ene click reactions.

4.3. Propagation Step: Role of Phenylthio Radicals

It can be argued that the rate of propagation and chain transfer steps of thiol-ene reactions can be controlled by the nature of the alkene and the radical as well as by the stability of carbon and the sulfur radicals which trigger the reaction. It is suggested by earlier articles [8,12,62] that propagation rate depends upon the electron density of alkene and the rate of chain transfer depends upon the stability of carbon radical. For this reason, in this study, different type of alkenes having various functional groups and para substituted thiophenols have been examined in detail. The energetics of eleven reactions

are investigated by the M06-2X/6-31++G(d,p) methodology (Table 4.5). All eleven reactions are enthalpically exothermic ranging between (-20.2 to -36.2 kcal/mol) and exergonic (-6.7 to -12.0 kcal/mol). The activation barriers of propagation step of all reactions show variation between 7.2 kcal/mol (4-methoxystyrene) to 13.3 kcal/mol (vinyl acetate) in terms of Gibbs free energy. The formation of radical intermediates is endergonic except for two reactions, reaction 7 (-1.4 kcal/mol) and reaction 8 (-0.5 kcal/mol). The relatively lower activation barrier of these outliers can lead to exothermic behaviour in the propagation step and the free energy of activation barrier (8.2 and 7.2 kcal/mol), respectively. When non-substituted pheylthio radical addition to different alkenes- first five reactions in Table 4.5 are taken into consideration, it can be argued that delocalization ability of radical intermediate pulls down the reaction exothermicity in addition to decreasing the activation barrier of the propagation reaction. Among these five reactions, relatively low activation barrier of reaction 4 can be result of the lower charge transfer energy (6.42 eV) for RS^- ene^+ (Table 4.5, Table 4.6). One of the reasons for low activation barrier of reaction 7 can be explained by its slightly low charge transfer energy (6.86 eV). However, low activation barrier and propagation step exothermicity of reaction 8 can be the result of resonance capability of the radical intermediate. In addition to resonance, for reaction 8, its low charge transfer energy (5.38 eV) is in line with the decrease in its reaction energetics. That's why, it can be asserted that variation in alkene functionality has considerable effect on activation barrier and reaction energetics of thiol-ene reactions as displayed in Table 4.5.

Table 4.5. Calculated activation barriers ($\Delta G^{\ddagger}$, $\Delta H^{\ddagger}$) and reaction energies (ΔG^o, ΔH^o) kcal/mol for propagation and chain transfer steps (M06-2X/6- 31++G(d,p)).

			Propagation				Chain Transfer				Overall	
Rxn	Radical	Alkene	$\Delta H^{\ddagger}_P$	$\Delta G^{\ddagger}_P$	ΔH^o_P	ΔG^o_P	$\Delta H^{\ddagger}_{CT}$	$\Delta G^{\ddagger}_{CT}$	ΔH^o_{CT}	ΔG^o_{CT}	ΔH^o_{rxn}	ΔG^o_{rxn}
1	$C_6H_5S^{\bullet}$	CH_2=CHPh	-3.8	9.1	-13.1	0.2	-1.6	10.6	-8.6	-8.5	-21.8	-8.3
2	$C_6H_5S^{\bullet}$	CH_2=C(Me)CO_2Me	-1.6	10.3	-11.9	0.4	-0.8	11.2	-8.3	-8.5	-20.2	-8.2
3	$C_6H_5S^{\bullet}$	CH_2=CH(CN)	1.2	12.6	-9.7	1.1	2.9	13.5	-11.8	-10.4	-21.4	-9.3
4	$C_6H_5S^{\bullet}$	CH_2=CH(OBu)	-3.7	11.4	-7.1	6.9	-8.1	8.1	-15.6	-10.9	-22.7	-4.0
5	$C_6H_5S^{\bullet}$	CH_2=CH(OC(O)Me)	-0.6	12.7	-7.6	6.5	-3.9	7.1	-19.2	-18.6	-26.8	-12.1
6	*p*-$MeOC_6H_5S^{\bullet}$	CH_2=C(Me)CO_2Me	-0.6	12.5	-10.2	3.0	-2.8	8.7	-23.3	-9.6	-33.5	-6.7
7	*p*-$NO_2C_6H_5S^{\bullet}$	CH_2=C(Me)CO_2Me	-3.6	8.2	-13.8	-1.4	-0.7	10.7	-22.4	-9.3	-36.2	-10.7
8	*p*-$ClC_6H_5S^{\bullet}$	p-MeO-PhCH=CH_2	-6.3	7.2	-14.4	-0.5	-5.4	7.6	-10.1	-8.7	-34.4	-7.2
9	*p*-$ClC_6H_5S^{\bullet}$	CH_2=C(Me)CO_2Me	-2.2	10.5	-12.2	0.9	-1.9	9.6	-22.2	-8.1	-24.5	-9.2
10	*p*-$ClC_6H_5S^{\bullet}$	CH_2=CH(OC(O)Me)	-1.0	12.5	-7.7	6.2	-5.8	9.1	-20.1	-18.2	-27.8	-12.0
11	*p*-$ClC_6H_5S^{\bullet}$	CH_2=CH(CN)	1.4	13.3	-9.3	2.0	2.0	13.6	-13.1	-11.2	-22.3	-9.2

Table 4.6. Calculated ionization potentials and electron affinities for alkenes and phenylthio radicals. Ionization potential, electron affinity, RS^- ene^+ and RS^+ ene^- energies are given in eV (M06-2X/6-31++G(d,p)).

Substrate	Ionization Potential	Electron Affinity	RS^- ene^+	RS^+ ene^-
CH_2=CHPh	8.5	0.5	6.2	9.3
CH_2=C(Me)CO_2Me	10.0	0.6	7.7	9.4
CH_2=CH(CN)	10.9	0.4	8.6	9.2
CH_2=CH(OBu)	8.7	0.8	6.4	9.6
CH_2=CH(OC(O)Me)	9.8	0.8	7.4	9.6
$C_6H_5S^\bullet$	8.8	-2.3		

Substrate	Ionization Potential	Electron Affinity	RS^- ene^+	RS^+ ene^-
p-MeO-PhCH=CH_2	7.9	0.8	5.4	9.5
CH_2=C(Me)CO_2Me	10.0	0.6	7.5	9.4
CH_2=CH(OC(O)Me)	9.8	0.8	7.2	9.6
CH_2=CH(CN)	10.9	0.4	8.4	9.2
p-Cl$C_6H_5S^\bullet$	8.8	-2.5		

Substrate	Ionization Potential	Electron Affinity	RS^- ene^+	RS^+ ene^-
$^1CH_2$=C(Me)CO_2Me	10.0	0.6	8.0	8.7
^{1}p-Me$OC_6H_5S^\bullet$	8.1	-2.0		
$^2CH_2$=C(Me)CO_2Me	10.0	0.6	6.9	10.3
^{2}p-$NO_2C_6H_5S^\bullet$	9.7	-3.1		

4.4. Propagation Step: Para-Substituted Phenylthio Radicals

It is highly important to study the effect of substituent on the phenylthio radical to detect factors that trigger the thiol-ene reactivity. In order to study this effect, four different well-known groups are used (-NO_2, -OMe, -Cl, -H) at the para position of the thiophenyl radical. It is proposed by Degirmenci *et al.* [63] that whereas the σ-withdrawing groups on sulfur radicals have destabilizing effect, the lone pair and the π acceptor groups on the sulfur radical have a stabilizing effect. In the same study, it is indicated that due to electronic characteristics of substituents on the sulfur centered radical -OMe to -NO_2 the deviation in the Zavitsas and Standard RSE is about 30 kcal/mol to 20 kcal/mol. In this study, there are four types of sulfur centered radicals and high energy change in RSE is not observed based on the substituent. However, high correlation (R^2 = 0.9857) between the RSE_{std} of the sulfur radical and spin density on the sulfur radical is obtained (Figure 4.4). The results in this study about the forming resonance structure of spin show consistency with a recent study [63]. The relationship between spin delocalization for various sulfur-centered radicals have shown a negative slope with RSE_{std}. When Figure 4.4 is considered, it can be apparently seen that spin density follows the rank MeO < H < Cl < NO_2, in parallel with the electron withdrawing feature of the substituents on the sulfur radical. Notwithstanding in the decreasing range of RSE_{std}, the reactivity of the radical is increasing. As shown for reactions 6 and 7 in Table 4.5, the phenylthio radical having electron withdrawing group (EWG) on it has low activation energy barrier due to the contribution of EWG substituents.

In this study, the effect of electronic characteristic of substrate is basically figured out at the addition reaction of sulfur centered radical to the alkene. The agreement (R^2 = 0.9479) between spin density and the activation barrier of propagation step is satisfactory Figure 4.5. This correlation explains that the stabilization of the sulfur centered radicals is provided by conjugated π-accepting groups. In light of these results, it can be concluded that spin densities not only have a remarkable influence on RSE_{std} but also on the activation barriers of the propagation step of thiol-ene reactions.

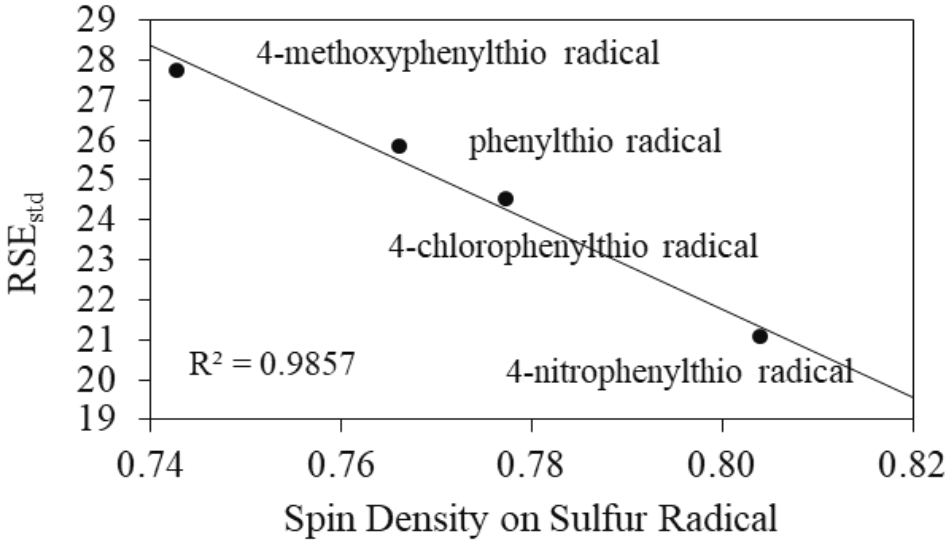

Figure 4.4. Correlation between RSE_{std} (kcal/mol) of 4 different para-substituted phenylthio radicals and spin density on sulfur radical (M06-2X/6-31++G(d,p)).

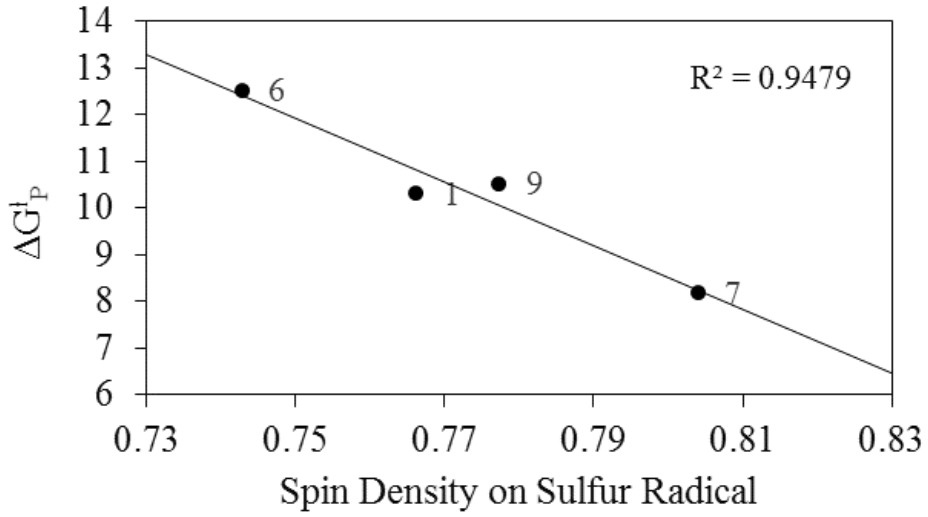

Figure 4.5. Correlation between $\Delta G^{\ddagger}_{P}$ (kcal/mol) and spin density on the sulfur radicals (M06-2X/6-31++G(d,p)).

4.5. Propagation Step: Role of Alkene Functionality

There are many studies where the addition of the carbon centered radical to alkenes has been studied experimentally [64,65] and computationally [28,66]. Even though the main factors that affect the reactivity of the carbon centered radical are well known,

knowledge about the reactivity of sulfur centered radical is highly limited. After addition of thiyl radical to the alkene, the carbon-carbon π bond is broken and a new carbon-sulfur bond forms. The length of the forming S-C bond distances at the transition state (Table 4.7) is well correlated (R^2 = 0.9135) with the enthalpy of the propagation step (Figure 4.6). Hammond's postulate [67] is obeyed as discussed in recent theoretical studies [24,29]. The addition of phenylthio radical to 4-methoxystyrene being the earliest transition state, it has the highest reaction enthalpy (ΔH^o_p = -14.36 kcal/mol), and the longest S-C distance at the transition state (2.44 Å). Moreover, 4-nitrophenylthio radical addition to methyl methacrylate (reaction 7) and phenylthio radical addition to styrene (reaction 1) have lower free energies of activation (8.2 and 9.1 kcal/mol) and longer S-C distance at the transition state (2.45 Å and 2.44 Å), respectively.

Table 4.7. Propagation transition state geometries of 11 thiol-ene reactions (M06-2X/6-31++G(d,p)).

Rxn	Propagation Step
1	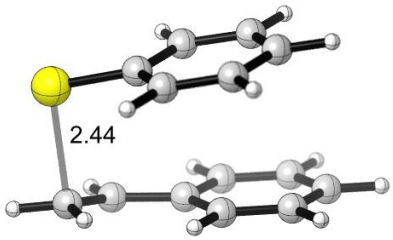
2	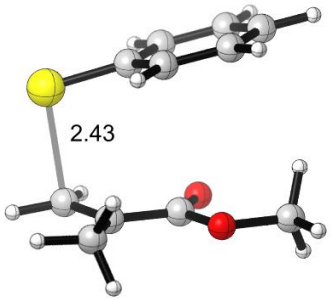
3	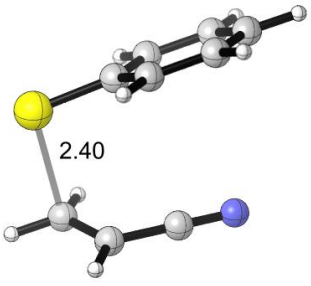

Table 4.7. Propagation transition state geometries of 11 thiol-ene reactions (M06-2X/6-31++G(d,p)) (cont.).

Rxn	Propagation Step
4	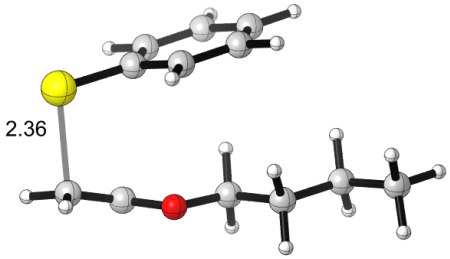
5	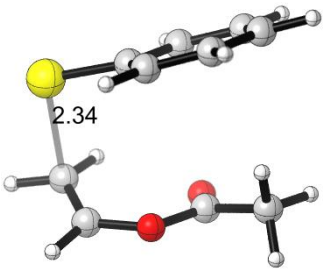
6	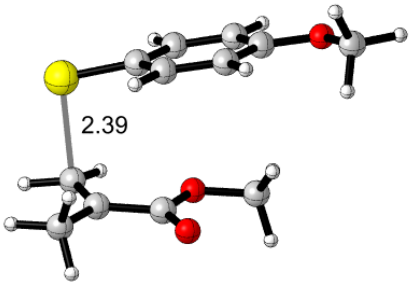
7	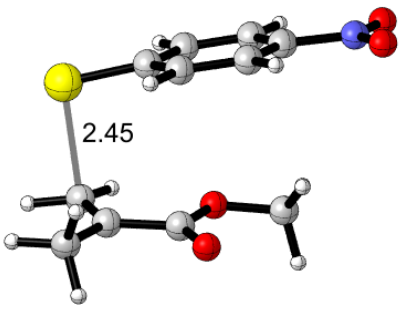
8	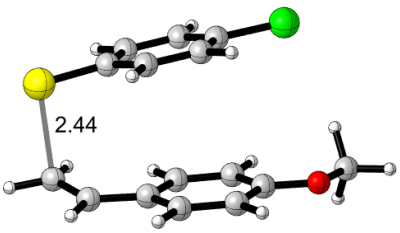

Table 4.7. Propagation transition state geometries of 11 thiol-ene reactions (M06-2X/6-31++G(d,p)) (cont.).

Rxn	Propagation Step
9	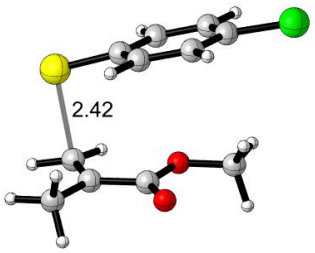
10	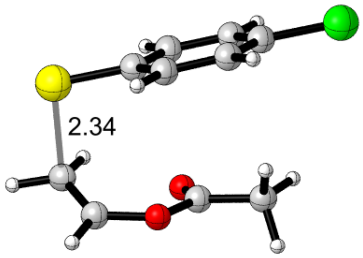
11	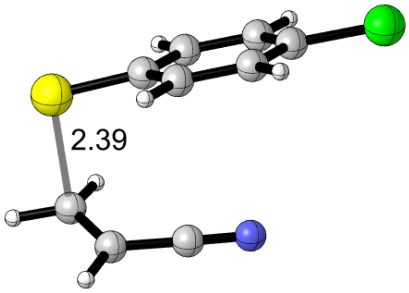

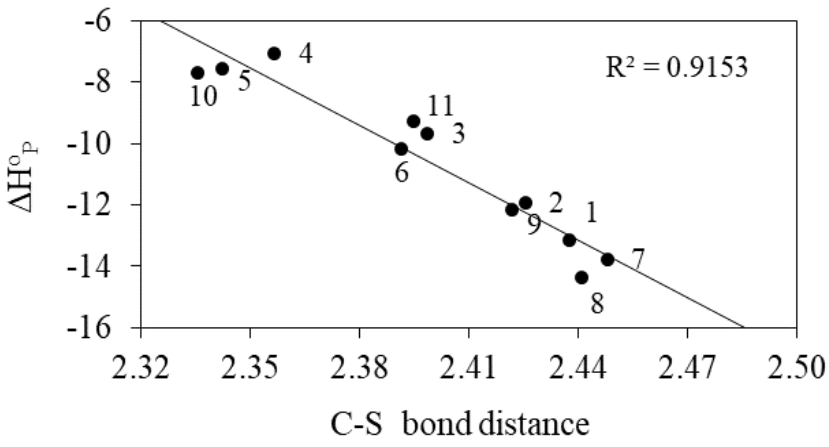

Figure 4.6. Relationship between ΔH^{o}_{p} (kcal/mol) and carbon-sulfur bond distances (Å) at the propagation transition state (M06-2X/6-31++G(d,p)).

In spite of the presence of a correlation between the forming bond distances and the reaction enthalpies, a correlation between the reaction enthalpies and the activation barriers for the same set of reactions is missing. These findings are reminiscent of the contribution of polar or nonpolar effects in the transition states for these sets of reactions. Figure 4.7 indicates that an Evans−Polanyi relationship [68] holds for this series of thiol−ene propagation reactions (R^2 = 0.9415) except that the outliers (reactions 4,5 and 10) are found to be more exothermic than expected. Figure 4.8 displays the same correlation with the outliers, the latter have an electron donor oxygen atom next to the C=C double bond, the corresponding intermediates are more destabilized -have higher barriers- than the other alkenes which possess electron withdrawing groups.

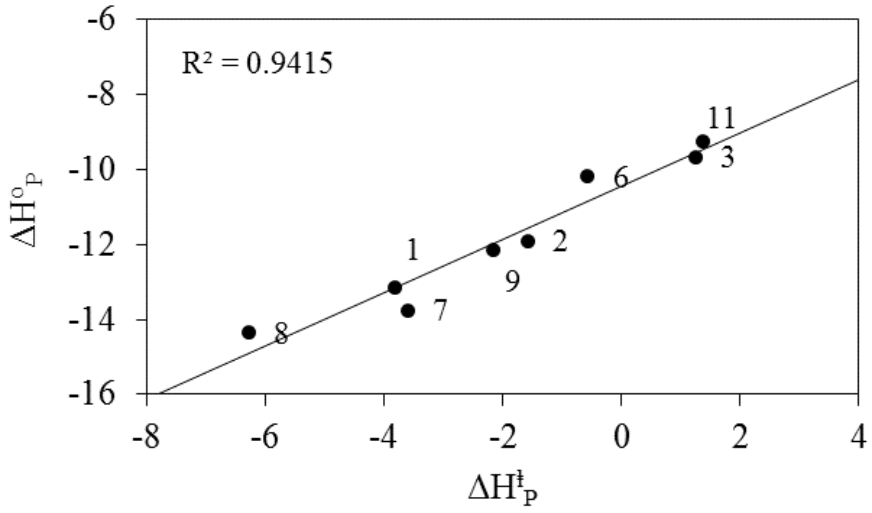

Figure 4.7. Correlation of ΔH^{o}_{P} (kcal/mol) versus $\Delta H^{‡}_{P}$ (kcal/mol) for the addition of phenylthio radical to the alkenes (M06-2X/6-31++G(d,p)).

It is also noteworthy to understand the reactivity of the alkene by monitoring the relationship between the RSE (Table 4.8) of the carbon centered radical intermediate and the singlet-triplet gap (S-T gap) (Table 4.9). RSE and S-T gap exhibit a reasonable correlation (R^2=0.8745) (Figure 4.9) with one outlier which when included decreases the correlation coefficient to 0.5855 (Figure 4.10). The S-T gap of the alkene represents the π-π* excitation energy and the π-bond strength of the alkene can be predicted by taking into consideration its S-T gap energy. The correlation coefficient between the Gibbs free energy of activation for the propagation step and the S-T gap is 0.8045 (Figure 4.11) 4-

methoxystyrene (reaction 9) has the lowest S-T gap (2.71 eV) and the lowest enthalpy of activation (-6.3 kcal/mol) as well as the lowest reaction enthalpy (-14.4 kcal/mol).

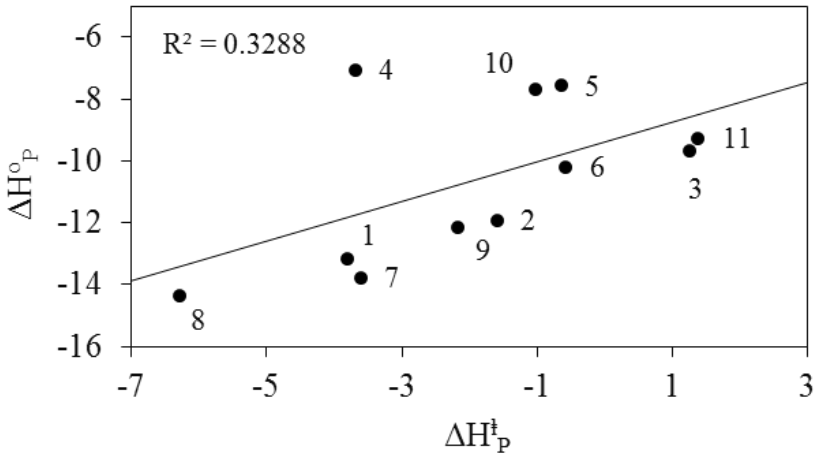

Figure 4.8. Correlation between ΔH^{o}_{P} (kcal/mol) and $\Delta H^{\ddagger}_{P}$ (kcal/mol) (M06-2X/6-31++G(d,p)).

Furthermore, the radical stabilization energy of the intermediate radical has the second highest RSE_z (13.1 kcal/mol). In reaction 5, vinyl acetate has one of the highest S-T gap (4.5 eV) and its intermediate has the lowest RSE_z (2.1 kcal/mol), it also has the second highest free energy of activation (12.7 kcal/mol). The same trend is followed for the other four reactions which have the same type of radical and different types of alkenes as reactants. Therefore, alkenes having high S-T energy gaps have high exothermicities and low activation barriers for propagation.

Table 4.8. Radical stabilization energies (kcal/mol) for phenylthiol radicals and carbon centered radical intermediates (M06-2X/6-31++G(d,p)).

		Phenylthio radical		Carbon intermediate radical	
radical	substrate	RSE_{std}	RSE_z	RSE_{std}	RSE_z
$C_6H_5S^{\bullet}$	CH_2=CHPh	25.8	21.4	17.1	13.2
$C_6H_5S^{\bullet}$	CH_2=C(Me)CO_2Me	25.8	21.4	16.3	11.9
$C_6H_5S^{\bullet}$	CH_2=CH(CN)	25.8	21.4	14.1	10.6
$C_6H_5S^{\bullet}$	CH_2=CH(OBu)	25.8	21.4	13.8	7.1
$C_6H_5S^{\bullet}$	CH_2=CH(OC(O)Me)	25.8	21.4	6.6	2.1
p-$MeOC_6H_5S^{\bullet}$	CH_2=C(Me)CO_2Me	29.9	27.8	16.8	12.4
p-$NO_2C_6H_5S^{\bullet}$	CH_2=C(Me)CO_2Me	24.8	21.1	16.2	11.5
p-$ClC_6H_5S^{\bullet}$	p-MeO-PhCH=CH_2	26.9	24.5	16.8	13.1
p-$ClC_6H_5S^{\bullet}$	CH_2=C(Me)CO_2Me	26.9	24.5	16.9	12.0
p-$ClC_6H_5S^{\bullet}$	CH_2=CH(OC(O)Me)	26.9	24.5	6.8	2.3
p-$ClC_6H_5S^{\bullet}$	CH_2=CH(CN)	26.9	24.5	13.8	10.4

Table 4.9. Singlet triplet gap for alkenes (eV), and electron density on C1 atom (NPA) (M06-2X/6-31++G(d,p)).

Substrate	S-T Gap	Electron Density on C1 Atom
CH_2=CHPh	3.65	-0.41
CH_2=C(Me)CO_2Me	3.96	-0.36
CH_2=CH(CN)	4.02	-0.34
CH_2=CH(OC(O)Me)	4.54	-0.43
CH_2=CH(OBu)	4.46	-0.60
p-MeO-PhCH=CH_2	2.71	-0.51

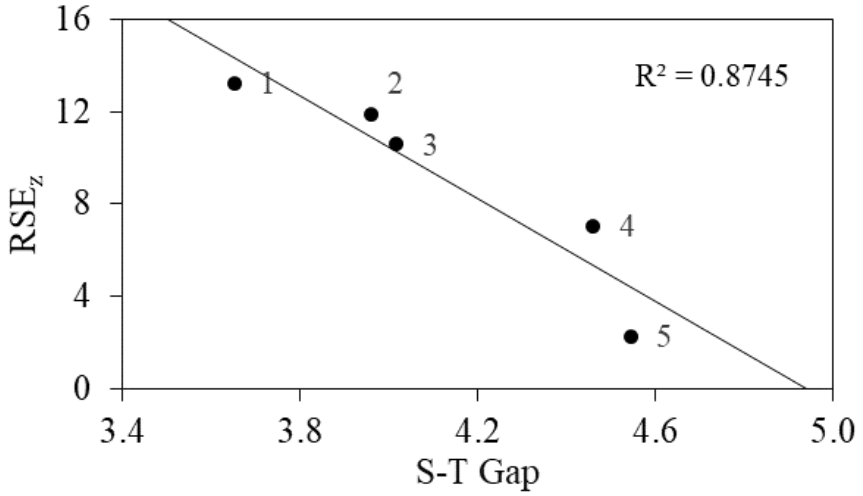

Figure 4.9. Correlation between RSE_z (kcal/mol) of carbon centered radical intermediate and S-T gap (eV) for alkenes without outliers (M06-2X/6-31++G(d,p)).

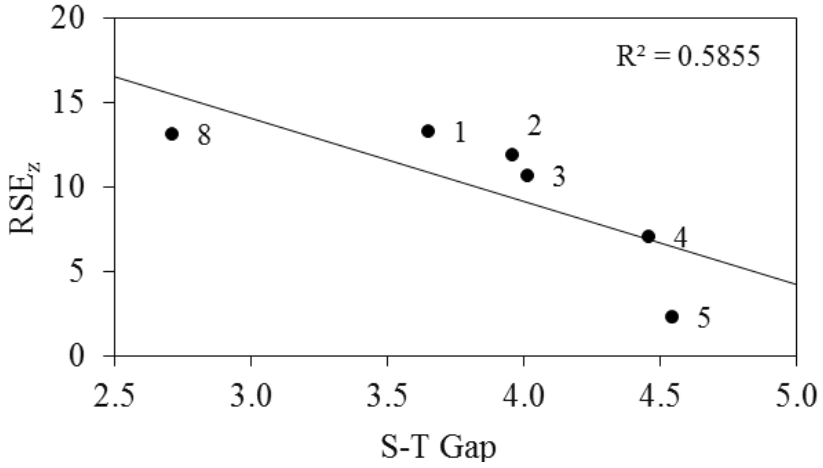

Figure 4.10. Correlation between RSE_z (kcal/mol) of carbon centered radical intermediate and S-T gap (eV) for alkenes (M06-2X/6-31++G(d,p)).

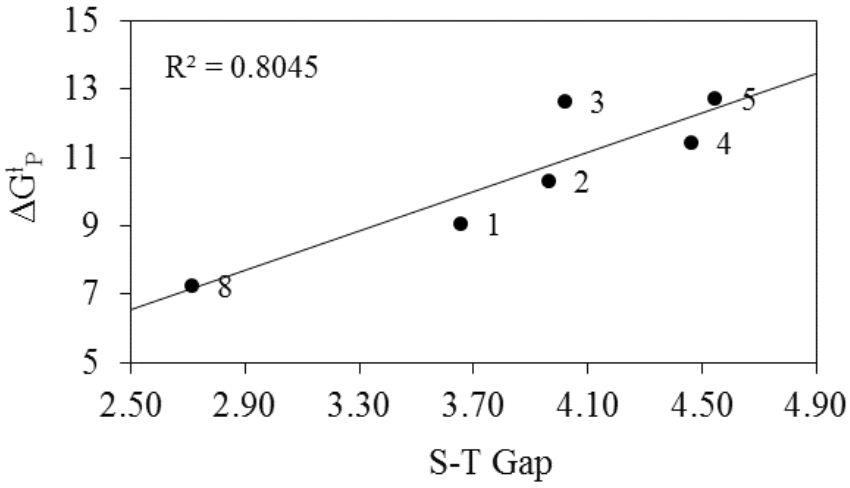

Figure 4.11. Correlation between $\Delta G^{\ddagger}_P$ (kcal/mol) and S-T gap (eV) for the alkenes (M06-2X/6-31++G(d,p)).

Further assessment to this approach was carried out in another theoretical study where low activation barriers were obtained by modeling alkyl thiyl radical additions to thioketones [29]. In the same study it has been emphasized that high SOMO energy of the radical and low energy of the π* orbital of the substrate can lead to resonance interaction in the transition state. In this study, we observe that the SOMO energies of the sulfur centered phenylthio radicals have higher SOMO energies than their carbon centered radical intermediates (Table 4.10). Reactions 2, 6, 7, 9 are chosen to investigate the relationship between the SOMO energies of phenylthio radicals and the activation barriers of the propagation step. The reactions have been chosen because they all have the same alkene (methyl methacrylate) in this way eliminating the errors that may emerge from the effect of the alkene type. High correlation is obtained for these series of reactions (R^2 = 0.9806) (Figure 4.12).

Table 4.10. SOMO energies of phenylthiol radicals and their carbon centered radical intermediates (Hartrees, M06-2X/6-31++G(d,p)).

Rxn	X	Phenylthio Radical	Carbon Centered Radical
2	H	-0.28635	-0.25675
6	MeO	-0.26727	-0.26647
7	NO_2	-0.31602	-0.28006
9	Cl	-0.28682	-0.27226

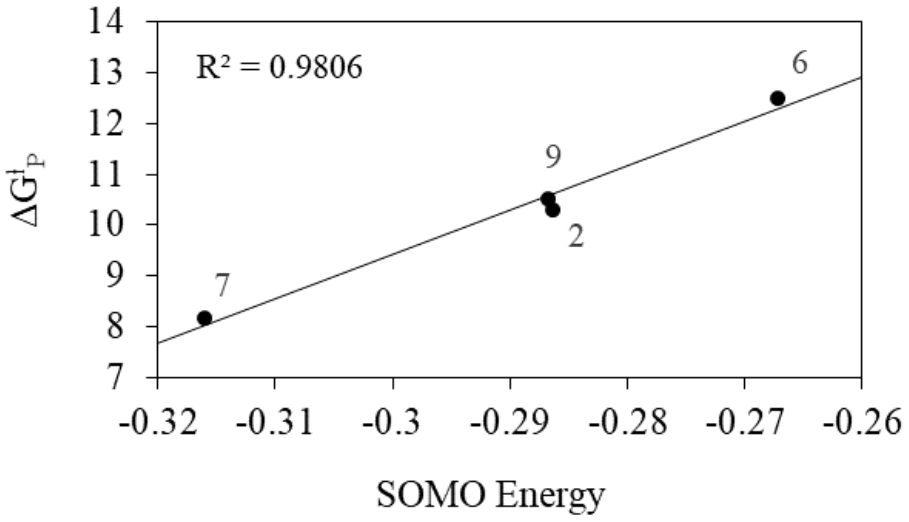

Figure 4.12. Correlation between $\Delta G^{\ddagger}_{P}$ (kcal/mol) and SOMO energies (a.u.) of phenylthio radicals (M06-2X/6-31++G(d,p)).

Bowman's experimental study reports that the rate of propagation for the thiyl radical addition to the alkene is mainly controlled by the electron density on the alkene [12]. However, a recent theoretical study has claimed that direct correlation between the propagation rate and the electron density is not valid [24]. In this study we show that, in a small set of reactions, there is a weak correlation between the enthalpy of activation for propagation and the electron density on C1 (R^2 = 0.1096) (Figure 4.13) with the exception of two outliers vinyl ether (reaction 4) and vinyl acetate (reaction 5). The characteristics of these two outliers can be rationalized by indicating the presence of the heteroatom next to the carbon-carbon double bond. Most probably, the oxygen atom is responsible for the higher electron density on C1 atom because of the mesomeric electron-donating properties of the oxygen atom.

Moreover, the increase in the activation barrier may be attributed to a late transition state (almost 0.1 Å difference) for reactions 4 and 5 (Table 4.11). When these outliers are taken out, the correlation is higher as claimed by Bowman [12] (R^2 = 0.9406) (Figure 4.14).

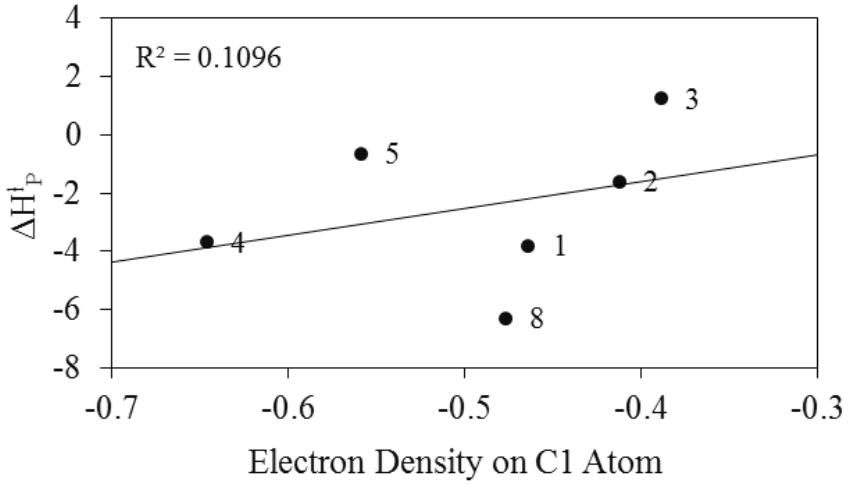

Figure 4.13. Correlation between $\Delta H^{\ddagger}_{P}$ (kcal/mol) and electron density on C1 atom of alkenes (M06-2X/6-31++G(d,p)).

The electronic configuration of the propagation state may influence the enthalpy of the activation barrier. Two polar charge transfer configurations are determined for each reaction. Table 4.11 displays the calculated energies of charge transfer configurations; these energies are determined by using the ionization potentials and electron affinities of both radicals and alkenes.

Table 4.11. Calculated energies (eV) of charge transfer configurations for eleven reactions with the S-C bond distances (Å) at the transition states (M06-2X/6-31++G(d,p)).

Rxn	Radical	Alkene	$RS^{-}ene^{+}$	$RS^{+}ene^{-}$	S-C
1	$C_6H_5S^{\bullet}$	CH_2=CHPh	6.23	9.33	2.44
2	$C_6H_5S^{\bullet}$	CH_2=C(Me)CO_2Me	7.70	9.44	2.43
3	$C_6H_5S^{\bullet}$	CH_2=CH(CN)	8.61	9.19	2.40
4	$C_6H_5S^{\bullet}$	CH_2=CH(OBu)	6.42	9.59	2.36
5	$C_6H_5S^{\bullet}$	CH_2=CH(OC(O)Me)	7.44	9.59	2.34
6	*p*-$MeOC_6H_5S^{\bullet}$	CH_2=C(Me)CO_2Me	7.97	8.71	2.39
7	*p*-$NO_2C_6H_5S^{\bullet}$	CH_2=C(Me)CO_2Me	6.86	10.30	2.45
8	*p*-$ClC_6H_5S^{\bullet}$	p-MeO-PhCH=CH_2	5.38	9.54	2.44
9	*p*-$ClC_6H_5S^{\bullet}$	CH_2=C(Me)CO_2Me	7.47	9.41	2.42
10	*p*-$ClC_6H_5S^{\bullet}$	CH_2=CH(OC(O)Me)	7.22	9.57	2.34
11	*p*-$ClC_6H_5S^{\bullet}$	CH_2=CH(CN)	8.38	9.16	2.39

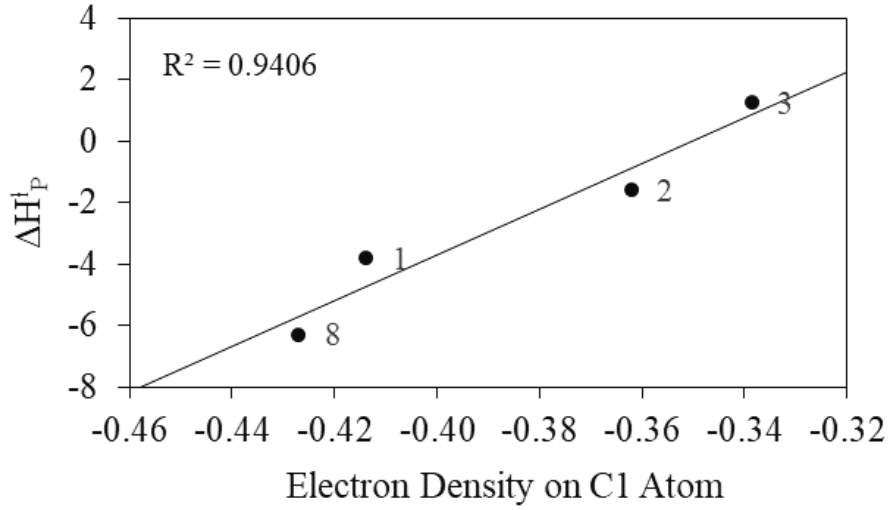

Figure 4.14. Correlation between $\Delta H^{\ddagger}_{P}$ (kcal/mol) and electron density on C1 atom without the outliers (M06-2X/6-31++G(d,p)).

For all the reactions, RS^{-} ene^{+} configurations have lower energy than RS^{+} ene^{-} configurations. Thus, the electrophilic characteristics of the phenylthio radicals dominate the reaction for the propagation step. Moreover, a reasonable correlation between the RS^{-} ene^{+} configurations and the activation enthalpies is established (Figure 4.15). As expected, the polar nature of the transition state affects strongly the activation barrier for propagation. Furthermore, the electrophilic nature of the sulfur-centered radicals is responsible of low charge transfer energy which leads to a decrease in the activation barrier.

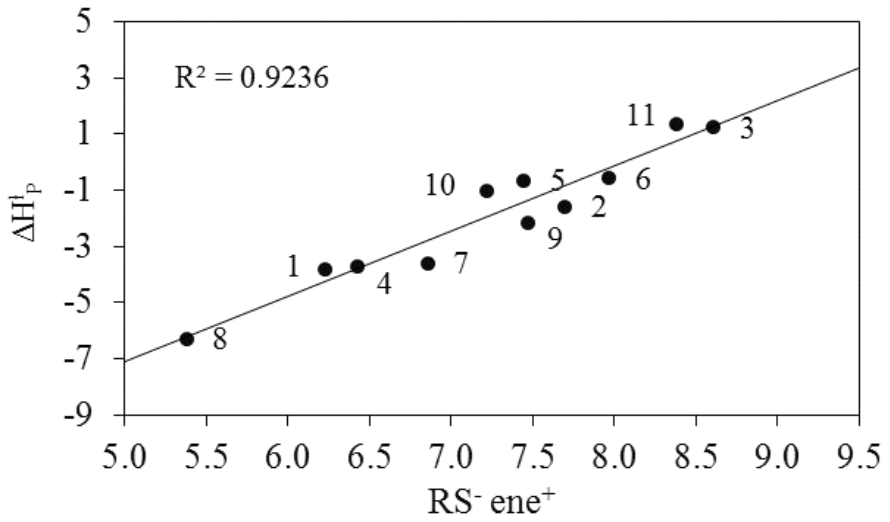

Figure 4.15. Relationship between $\Delta H^{\ddagger}_{P}$ (kcal/mol) and RS^{-} ene^{+} charge-transfer configurations (eV) for propagation steps (M06-2X/6-31++G(d,p)).

4.6. Chain Transfer

A subsequent reaction of the propagation step can be the abstraction of a hydrogen atom from thiophenol by the intermediate carbon-centred radical to yield a thioether and a phenylthio radical (Figure 1.2, Table 4.5). The newly formed sulfur centered radical shows a different behavior than the carbon centered radical thus both steps deserve careful analysis. The Gibbs free energy activation barriers of the chain transfer vary by nearly 6.5 kcal/mol.

Bowman and co-workers [12] have reported that chain transfer rate directly depends on the radical stability of the carbon radical at the intermediate structures. It is well-known that electronegative or electron-withdrawing groups for instance, -CF_3, -NO_2, -F, and -OC(O)R destabilize the carbon-centered radicals. On the other hand, electron-donating substituents such as -Me and -NH_2 stabilize them [69,70]. Destabilization due to the electron-withdrawing nature of the -$OC(O)CH_3$ (reactions 5 and 10) and –CN groups (reactions 3 and 11) on the radical center leads to relatively low exothermicities for the propagation reaction. On the other hand, the expected larger exothermicities for the chain transfer reaction of carbon-centered radicals which have electron-withdrawing groups couldn't be observed. Note that, the alkenes having electron donating groups such as -Me, -Ph, -PhOMe (reactions 1, 2, 6, 7, 8, 9) are more exothermic in the propagation reactions and chain transfer reactions except for reaction 8.

Furthermore, in addition to the effect of electron-donating and electron-withdrawing groups, the stability of carbon centered radical intermediate can be considered as another main property that has an effect on the chain transfer activation barrier. However, a correlation couldn't be established between radical stability (RSE_{std}) of the radical intermediate and the enthalpy of activation barrier of chain transfer because of the three effective outliers (reactions 4, 5, 10) (R^2 = 0.09) (Figure 4.16). The outliers have low RSE_{std} (13.8, 6.6, 6.8 kcal/mol) and low activation barriers for chain transfer) 8.1, 7.1, 9.1 kcal/mol), respectively. Overall, electron withdrawing groups decrease the stability of the carbon radical for these monomers more than expected. When outliers are ignored, a relatively high correlation is obtained as seen in Figure 4.17 (R^2 = 0.9198).

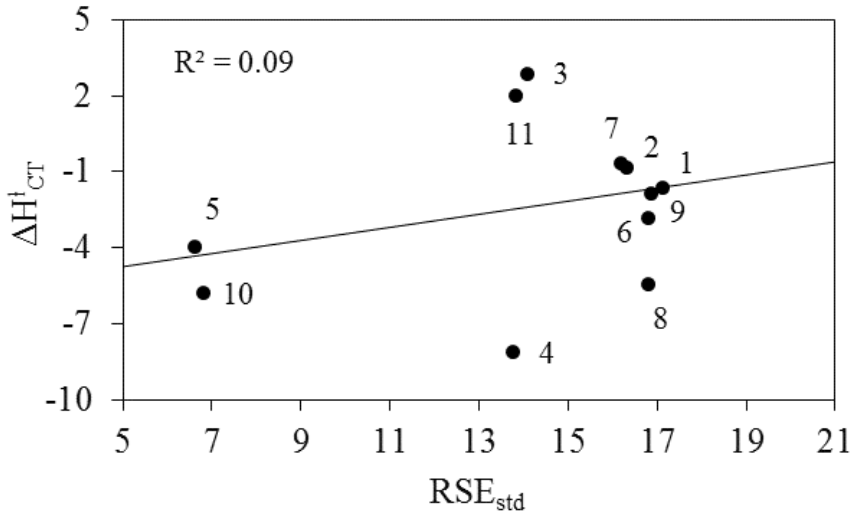

Figure 4.16. $\Delta H^{\ddagger}_{CT}$ (kcal/mol) versus standard RSE_{std} (kcal/mol) for carbon centered radicals (M06-2X/6-31++G(d,p)).

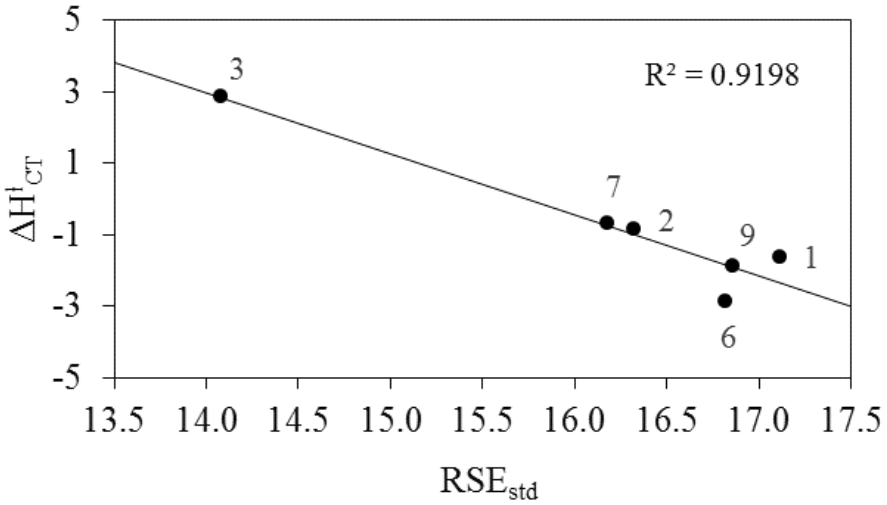

Figure 4.17. Correlation of $\Delta H^{\ddagger}_{CT}$ (kcal/mol) versus RSE_{std} (kcal/mol) for carbon centered radical intermediates without the outliers (M06-2X/6-31++G(d,p)).

In order to evaluate the transition states of the chain transfer reaction, the Evans-Polanyi relationship [68] for this reaction was considered (Figure 4.18) however a correlation between $\Delta H^{\ddagger}_{CT}$ and ΔH^{o}_{CT} has not been established . This result is at odds with a previous study for the abstraction of a hydrogen atom from methyl mercaptan where a reasonable correlation (R^2=0.83) between the reaction enthalpy and the enthalpy of activation was derived [24]. In our set of thiols, the chain transfer reaction can be affected by steric factors, spin delocalization, contribution of the electron withdrawing or donating groups, π-π interactions and also possible H atom-π interactions or lone pair electrons-π

interactions while not all these effects are present in the reaction of methyl mercaptan. Note that, bond distances between hydrogen and heavy atoms (C-H, S-H) at the transition states of the chain transfer reactions and the corresponding reaction Gibbs free energies are well correlated (R^2 = 0.8078 and 0.6888 respectively) (Figure 4.19 and Figure 4.20).

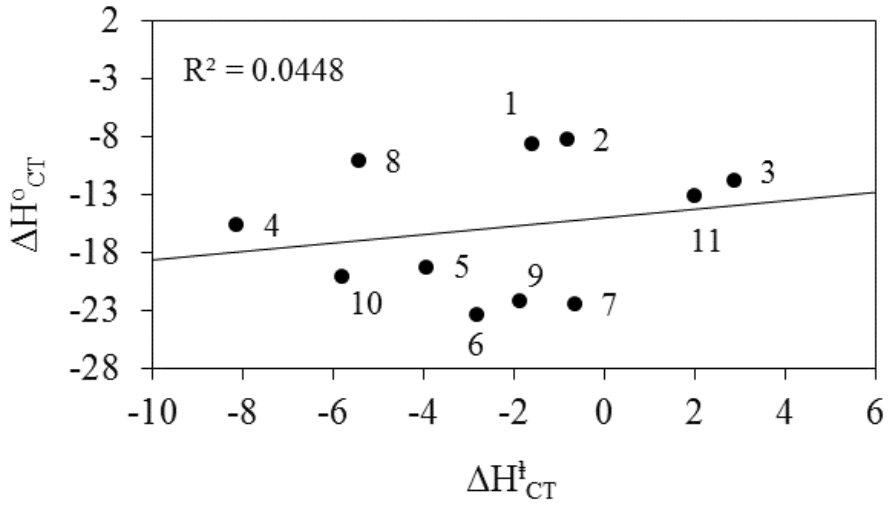

Figure 4.18. Correlation of ΔH^{o}_{CT} (kcal/mol) versus $\Delta H^{‡}_{CT}$ (kcal/mol) for chain transfer reactions (M06-2X/6-31++G(d,p)).

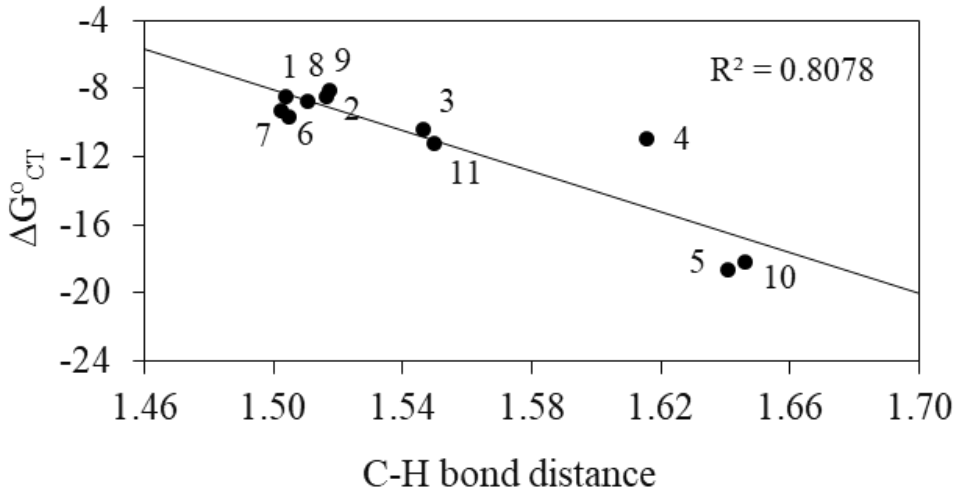

Figure 4.19. ΔG^{o}_{CT} (kcal/mol) versus C-H bond distance (Å) in chain transfer transition states (M06-2X/6-31++G(d,p)).

The transition structures of chain transfer reactions have sandwich-like structures where there are favorable interactions either between the phenyl groups (reactions 1 and 8) or between the phenyl groups and the lone pairs of the heteroatoms (reactions 2, 3, 4, 5, 6,

7, 9, 10, 11). Overall the activation barriers of chain transfer reactions are lower than the ones for the propagation reaction. Strong favorable π interactions in the chain transfer transition states can alter significantly k_{CT} and the k_P/k_{CT} ratio. (Table 4.12). The presence of hetero atoms or polar groups on the thiol structures allows the modification of the k_P/k_{CT} ratio thus the overall order of the reaction (Table 4.12).

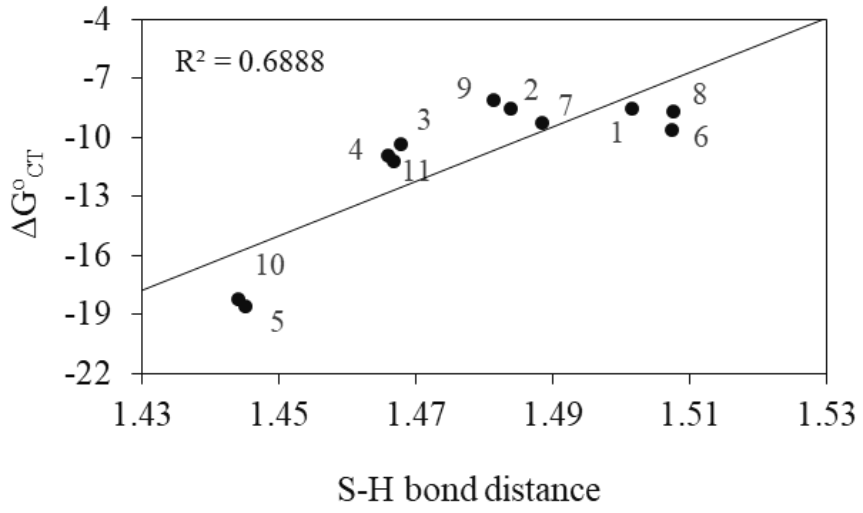

Figure 4.20. ΔG^{o}_{CT} (kcal/mol) versus S-H bond distance (Å) in chain transfer transition states (M06-2X/6-31++G(d,p)).

Table 4.12. Dipole moment (μ), $\Delta H^{\ddagger}_{CT}$, $\Delta G^{\ddagger}_{CT}$ for chain transfer reactions (M06-2X/6-31++G(d,p)).

	Radical	Alkene	Dipole Moment	$\Delta H^{\ddagger}_{CT}$	$\Delta G^{\ddagger}_{CT}$
1	$C_6H_5S^{\bullet}$	CH_2=CHPh	4.07	-1.62	10.63
2	$C_6H_5S^{\bullet}$	CH_2=C(Me)CO_2Me	3.11	-0.84	11.17
3	$C_6H_5S^{\bullet}$	CH_2=CH(CN)	1.42	2.87	13.48
4	$C_6H_5S^{\bullet}$	CH_2=CH(OBu)	3.33	-8.14	8.05
5	$C_6H_5S^{\bullet}$	CH_2=CH(OC(O)Me)	3.79	-3.94	7.12
6	*p*-$MeOC_6H_5S^{\bullet}$	CH_2=C(Me)CO_2Me	4.32	-2.84	8.74
7	*p*-$NO_2C_6H_5S^{\bullet}$	CH_2=C(Me)CO_2Me	7.05	-0.67	10.74
8	*p*-$ClC_6H_5S^{\bullet}$	p-MeO-PhCH=CH_2	1.95	-5.45	7.57
9	*p*-$ClC_6H_5S^{\bullet}$	CH_2=C(Me)CO_2Me	1.52	-1.87	9.64
10	*p*-$ClC_6H_5S^{\bullet}$	CH_2=CH(OC(O)Me)	1.81	-5.81	9.07
11	*p*-$ClC_6H_5S^{\bullet}$	CH_2=CH(CN)	3.03	1.99	13.60

Table 4.13. Chain-transfer transition state geometries of 11 thiol-ene reactions (M06-2X/6-31++G(d,p)).

Rxn	Chain Transfer Step
1	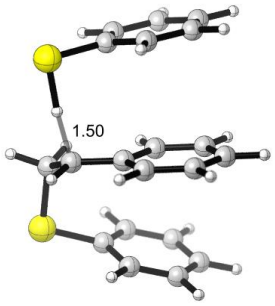
2	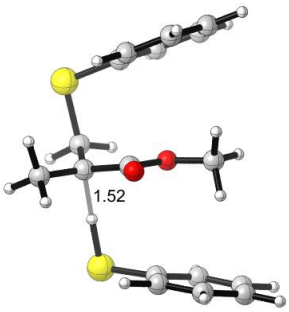
3	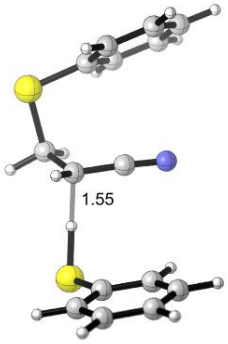
4	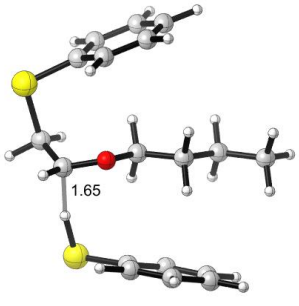

Table 4.13. Chain-transfer transition state geometries of 11 thiol-ene reactions (M06-2X/6-31++G(d,p)) (cont.).

Rxn	Chain Transfer Step
5	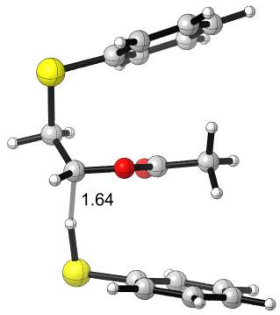
6	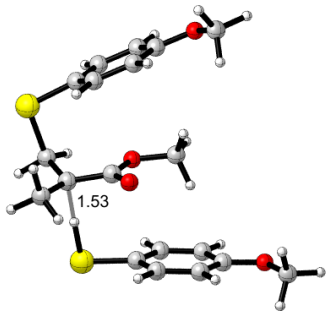
7	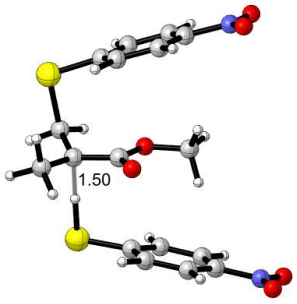
8	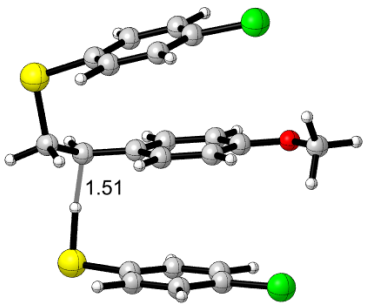

Table 4.13. Chain-transfer transition state geometries of 11 thiol-ene reactions (M06-2X/6-31++G(d,p)) (cont.).

9	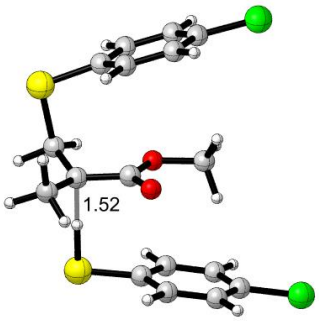
10	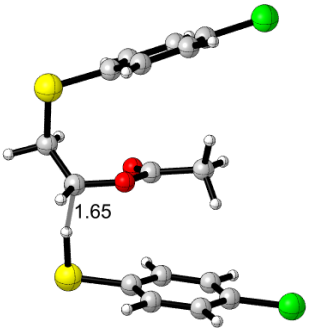
11	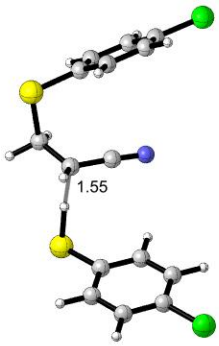

4.7. Reaction Rates

As pointed out so far in various studies,[14,15,16,18] the crucial point for thiol-ene reactions and their applications is the k_P to k_{CT} ratio (Table 4.14). Based on the Gibbs free energy activation barriers and the Gibbs free reaction energies (Table 4.5) the ranking of the forward and reverse rate constants for propagation (2.66E+04 to 7.61E+08) and chain transfer reactions (1.67E+04 to 9.28E+08) is quite similar.

Table 4.14. Forward and Reverse Rate Constants for Propagation and Chain Transfer Steps for Thiol-ene Reactions (k_P/k_{CT}) (M06-2X/6-31++G(d,p)).

			Propagation (k_P)		Chain Transfer (k_{CT})		
Rxn	Radical	Alkene	Forward	Reverse	Forward	Reverse	k_P/k_{CT}
1	$C_6H_5S^{\bullet}$	CH_2=CHPh	3.54E+07	5.31E+07	2.48E+06	1.45E+00	14.28810
2	$C_6H_5S^{\bullet}$	CH_2=C(Me)CO_2Me	4.35E+06	7.99E+06	1.00E+06	5.74E-01	4.34943
3	$C_6H_5S^{\bullet}$	CH_2=CH(CN)	8.37E+04	5.56E+05	2.02E+04	5.00E-04	4.13823
4	$C_6H_5S^{\bullet}$	CH_2=CH(OBu)	6.56E+05	7.57E+10	1.93E+08	1.88E+00	0.00340
5	$C_6H_5S^{\bullet}$	CH_2=CH(OC(O)Me)	7.34E+04	4.09E+09	9.28E+08	2.19E-05	0.00008
6	*p*-$MeOC_6H_5S^{\bullet}$	CH_2=C(Me)CO_2Me	1.03E+05	1.52E+07	6.02E+07	5.33E+00	0.00171
7	*p*-$NO_2C_6H_5S^{\bullet}$	CH_2=C(Me)CO_2Me	1.56E+08	1.48E+07	2.08E+06	3.33E-01	74.87921
9	*p*-$ClC_6H_5S^{\bullet}$	p-MeO-PhCH=CH_2	7.61E+08	3.14E+08	4.37E+08	1.84E+02	1.74005
8	*p*-$ClC_6H_5S^{\bullet}$	CH_2=C(Me)CO_2Me	3.03E+06	1.35E+07	1.32E+07	1.44E+01	0.22919
10	*p*-$ClC_6H_5S^{\bullet}$	CH_2=CH(OC(O)Me)	9.92E+04	3.65E+09	3.47E+07	1.55E-06	0.00286
11	*p*-$ClC_6H_5S^{\bullet}$	CH_2=CH(CN)	2.66E+04	8.36E+05	1.67E+04	9.81E-05	1.59700

As mentioned earlier, the k_P/k_{CT} ratio has an importance on thiol-ene reactions (Figure 1.3). If the ratio is higher than 1.0 rate the limiting step is k_{CT}, if it is lower than 1.0 the rate limiting step is k_P. Phenylthio radical addition to styrene (reaction 1) and 4-nitrophenylthio radical addition to methyl methacrylate (reaction 7) have ratios greater than 1.0. The reactions of phenylthio radical addition to methyl methacrylate, acrylonitrile (reaction 2,3) and the reaction of 4-chloropheyltio radical addition to acrylonitrile (reaction 11) have k_P/k_{CT} values close to 1, the other reactions have k_P/k_{CT} values lower than 1.0. However, if k_P and k_{CT} values are similar and the reverse propagation rate k_{-P} is higher than the forward chain transfer rate, it is hard to describe the overall reaction kinetics accurately as in the case of reactions 1 and 3.

In the set of reactions considered in this study, all the propagation reactions seem to be significantly reversible except for 4-nitrophenylthio radical addition to methyl methacrylate (equilibrium ratio is about 10.54). The relatively low radical stabilization energy of sulfur-centered radical of this reaction can be responsible for this behavior (Table 4.8). Some experimental studies have already revealed that thiyl radical addition is thermodynamically reversible for thiyl radical and electron rich alkenes [6,71,72,73,74].

This phenomenon has already been proved for methyl thiyl addition to vinyl ether, vinyl silane and allyl ether [24]. In this study, except for 4-nitrophenylthio radical addition to methyl methacrylate all other reactions can be significantly affected by high reversibility of the propagation reaction. Among the ten reversible reactions, three (reactions 4, 5 and 10) have similar tendency and high reversibility, the reverse propagation rate for these reactions is about 5 orders of magnitude larger than the forward addition reaction. Especially, the overall reaction rate of vinyl acetate (reaction 5,10) and butylvinylether (reaction 4) can be expected to be slower than the other monomers due to the β C-S scission. Equilibrations of these three reactions at the propagation step leads to the formation of sulfur radicals because of the weak S-C bond. In the case of methyl mercaptan [24], the intermediate radical can play an important role for the reaction. But, in the phenylthiol derivatives, both transition states for the addition and chain transfer reaction can be significantly influenced by polar effects. Therefore, radical stability of the intermediate products alone is not enough to explain overall thiol-ene reaction. All forward chain transfer reactions have more than 5 orders of magnitude larger rate constants than the reverse ones due to the significant radical stabilization energy differences between phenylthio radicals in the product and the carbon-centered radicals as intermediate product (Table 4.8).

Individual rate constants for the propagation step of a series of reactions have been measured experimentally by Ito and co-workers [25,75,76,77]. The absolute rate constants are determined by the SRS flash photolysis method [77] while the relative rate constants have been evaluated by the spin-trapping ESR method [78]. In this study, a high correlation coefficient ($R^2 = 0.8447$) between experimental and theoretical results has been assessed even though the experimental polymerization reactions take place in bulk and the theoretical calculations are evaluated in the gas phase. The logarithmic scale of this correlation is displayed in Figure 4.21. In contrast to the recently published theoretical study [24], a sound correlation between the stability of the formed intermediate carbon-centered radical and the chain transfer activation barrier couldn't be established. Note that due to the lack of thiol functionality a correlation between the stability of the formed intermediate carbon-centered radical and the chain transfer activation barrier has been established by Northrop and co-workers [24].

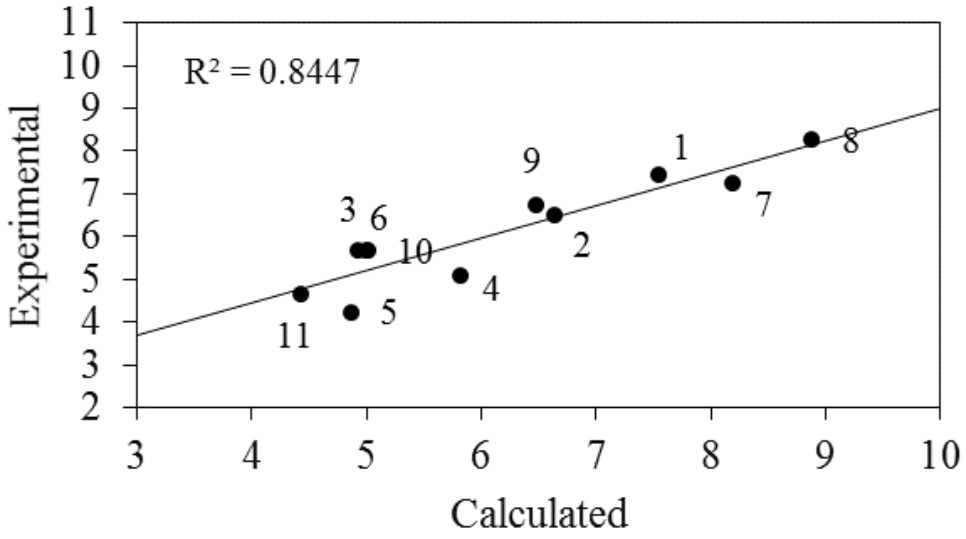

Figure 4.21. Comparison of experimental and calculated rate constants of propagation steps (logarithmic scale).

5. THIOL-ALKYL REACTIONS

5.1. Computational Procedure

Due to the success of the M06-2X/6-31++G(d,p) methodology in the first party of the thesis, the same methodology has been used to model the kinetics of thiol-alkyl reactions in solution. Rate constants are calculated by using equation 4.3 where, $k(T)$ is the reaction rate constant, R is universal gas constant (8.314 J mol^{-1} K^{-1}), $\kappa(T)$ is tunneling correction (for simplicity it is taken as 1), k_B is the Boltzmann constant (1.380658x10^{-23} J K^{-1}), T is the temperature (298.15 K), h is Planck's constant (6.6260755x10^{-34} J s), c^o is the standard unit of concentration (mol L^{-1}) (= $n/V = P^{\theta}/RT$), m is the molecularity of the reaction, and $\Delta G^{\ddagger}$is the Gibbs Free energy change between activated complex and reactants.

5.2. Solvent Effects and Hydrogen Atom Transfer in Aqueous Solutions

It is suggested that the equilibrium constant of carbon and sulfur centered radicals cannot be affected by the reaction media even if there is not a remarkable interaction that controls the activation barrier of the reaction [57]. It is reported that the rate of hydrogen abstraction reaction from hydrocarbons to thiyl radical increases in aqueous media [79]. However, it is shown that there is not a significant difference in solvents having low polarity, for example, THF and toluene [80]. Due to the fact that the remarkable importance of the reaction of thiyl radical in biological cell, several studies about the reactivity of thiyl radical in water have been published [39,79,81,82].

In this study, four different hydrogen abstraction reactions having experimental rate constants are modelled to understand the role of the solvent. Table 5.1 displays the calculated activation barriers of these reactions. 2D representation of reactants and calculated and experimental results [57] are displayed in Table 5.2. In the transition state structures shown in Table 5.3, H abstraction by the alkyl radicals takes place with a distance varying between 1.39 Å to 1.57 Å. The activation barriers for forward reactions vary between 8.37 to 14.66 kcal/mol, those for the backward reactions rank between 9.14

to 15.50 kcal/mol. Note that for the reactions 2 and 3, reverse reactions are faster than the forward reactions because of primary alkyl radicals abstract a hydrogen atom from thiols rapidly, secondary and tertiary alkyl radicals react more slowly probably due to their relative thermodynamic stability while the reverse reaction follows the opposite trend [57]. The calculated forward and reverse rate constants are tabulated in Table 5.2. Even if the experimental results are in the aqueous media, reactions energetics are investigated in gas phase and implicit water. The results have shown that the calculated rate constants are in the agreement with the experimental ones.

Table 5.1. Calculated activation barriers ($\Delta G^{\ddagger}$) and reaction energies (ΔG^{o}) for hydrogen abstraction reaction by alkyl radicals from thiols (M06-2X/6- 31++G(d,p)).

			Gas				Water				Acetonitrile	
			Forward		Reverse		Forward		Reverse		Forward	
Rxn	Thiol	Alkyl Radical	$\Delta G^{\ddagger}_P$	ΔG^{o}_P	$\Delta G^{\ddagger}_P$	ΔG^{o}_P	$\Delta G^{\ddagger}_P$	ΔG^{o}_P	$\Delta G^{\ddagger}_P$	ΔG^{o}_P	$\Delta G^{\ddagger}_P$	ΔG^{o}_P
1	Me_2**C**(OH)	PenSH	8.37	-7.13	15.50	7.13	8.41	-6.97	15.38	6.97		
2	Ph**C**H(OH)	$H_2N(CH_2)_2SH$	14.66	5.52	9.14	-5.52	15.15	5.97	9.18	-5.97		
3		$H_2N(CH_2)_2SH$	10.81	-0.44	11.24	0.44	15.96	0.40	15.56	0.40		
4		t-BuSH	8.71	-8.89			9.69	-8.33			9.72	-8.33

Table 5.2. Calculated and Experimental rate constants for thiol-alkyl reactions (M06-2X/6-31++G(d,p).

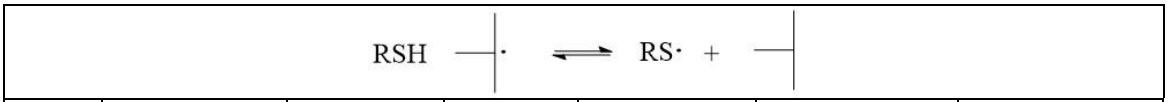

Rxn	Radical	Thiol	Media	k_H- Calculated k_{-H}- Calculated	k_H- Experimental	k_{-H}- Experimental
1	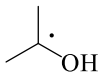	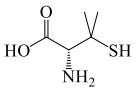	Gas Phase	1.13E+08 6.60E+02		
			Water	1.06E+08 8.19E+02	1.00E+08	1.00E+04

Table 5.2. Calculated and Experimental rate constants for thiol-alkyl reactions (M06-2X/6-31++G(d,p) (cont).

Rxn	Radical	Thiol	Media	k_H-Calculated k_{-H}-Calculated	k_H-Experimental	k_{-H}-Experimental
2	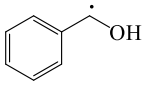	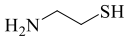	Gas Phase	2.78E+03 8.81E+05		
			Water	1.21E+03 6.05E+02		1.00E+07
3	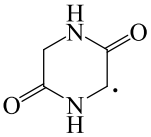	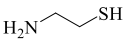	Gas Phase	1.84E+06 3.09E+07		
			Water	3.07E+02 2.88E+07		4.00E+05
4	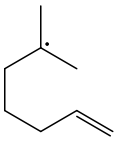		Gas Phase	6.35E+07 -		
			Water	1.22E+07 -	1.30E+07	
			CH3CN	1.15E+07 -	3.50E+06	

Table 5.3. Transition state geometries of thiol-alkyl reactions (M06-2X/6-31++G(d,p)).

Rxn	Gas Phase	Water	CH_3CN
1	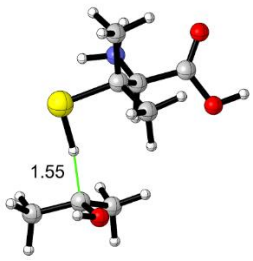	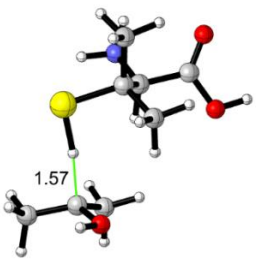	

Table 5.3. Transition state geometries of thiol-alkyl reactions (M06-2X/6-31++G(d,p)) (cont.).

2	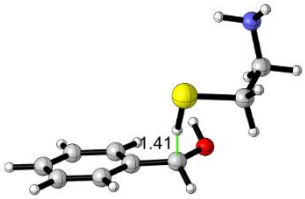	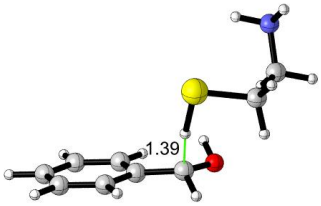	
3	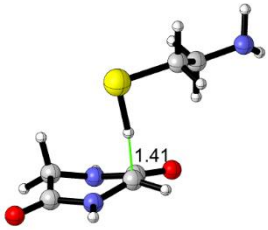	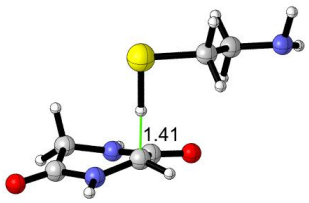	
4	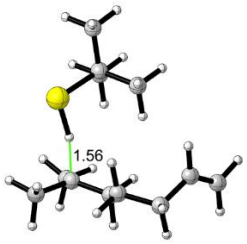	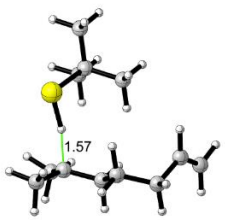	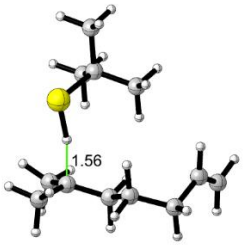

The effect of solvent polarity (H_2O, CH_3CN) is examined by modelling hydrogen abstraction reaction from *t*-BuSH to alkyl radical (reaction 4) and the rate constants are compared to the experimental rate constants [39]. Tables 5.2 demonstrates that the rates of H-transfer from alkyl thiols to alkyl radicals depend on the polarity of the solvent. In the hydrogen abstraction reaction between the different radicals, the solvent may affect the reaction energetics by stabilizing the reactants, transition state configuration (Table 5.3) or the products. In this thesis, the results show that the stabilization character of water is higher than acetonitrile for abstraction reaction from *t*-BuSH to alkyl radical as reported in previous experimental article [39]. For reaction 4, even if the amount of the stabilization energy for reactants and products in both water and acetonitrile is higher than transition state, it can be said that the stabilization energy differences between water and acetonitrile in the transition state is higher than the stabilization energy differences of reactants and products.

5.3. Conclusion and Future Work

The thiol-ene reaction mechanism was investigated with the DFT methodology for six different types of monomers and four different phenyl thiols. In spite of the numerous studies on the role of the ene functionality on the thiol-ene reaction, the essence of the thiol functionality on the mechanism has been elucidated for the first time by considering the substituent effects of the phenylthiol group by using the M06-2X/6-31++G(d,p) methodology. Among the factors which facilitate the propagation reaction, the electrophilic characteristics of the phenylthio radicals and the stability of the RS^{-} ene^{+} configuration was found to be more responsible than the S-T gaps of the ene functional groups. In our set of reactions, favorable intermolecular interactions have been detected at the chain transfer transition state structures. These interactions are the source of the deviation from the linear relationship between the stability of carbon radical and the activation barriers of chain transfer reaction. In this study, we emphasize the fact that the k_P/k_{CT} ratio is controlled not only by the alkene functionality but also by the thiol functionality. As a result, we have also demonstrated that the limiting reactions of the thiol-ene reaction mechanism can be altered from the propagation to chain transfer reaction by just changing substituents on the thiol group. This information can be useful for tailoring polymer structure that enables adjusting desirable physical and mechanical properties of polymer product without changing the alkene functionality.

In the set of thiol-alkyl reactions carried out in solvents with different polarities, the implicit solvation model seems to reproduce the experimental results in most cases. However, the set of reactions used is not sufficient to draw sound conclusions about this study. This part of the work is in progress, a larger set of reactions will be modelled in order to detect the role of solvent in thiol-alkyl reactions.

REFERENCES

1. Kolb, H.C., M.G. Finn, and K.B. Sharpless, “Click Chemistry: Diverse Chemical Function From A Few Good Reactions.”, *Angewandte Chemie - International Edition*, Vol. 40, pp. 2004–2021, 2001.

2. Binder, W.H., and R. Sachsenhofer, “‘Click’ Chemistry In Polymer And Materials Science.”, *Macromolecular Rapid Communications*, Vol. 28, pp. 15–54, 2007.

3. Binder, W.H., and R. Sachsenhofer, “‘Click’ Chemistry In Polymer And Material Science: An Update.”, *Macromolecular Rapid Communications*, Vol. 29, pp. 952–981.

4. Le Droumaguet, B., and K. Velonia, “Click Chemistry: A Powerful Tool To Create Polymer-based Macromolecular Chimeras.”, *Macromolecular Rapid Communications*, Vol. 29, pp. 1073–1089, 2008.

5. Posner, T., “Beiträge Zur Kenntniss Der Ungesättigten Verbindungen. II. Ueber Die Addition Von Mercaptanen An Ungesättigte Kohlenwasserstoffe.”, *Berichte der deutschen chemischen Gesellschaft*, Vol. 38, pp. 646–657, 1905.

6. Roper, T.M., C.A. Guymon, E.S. Jönsson, and C.E. Hoyle, “Influence Of The Alkene Structure On The Mechanism And Kinetics Of Thiol-alkene Photopolymerizations With Real-time Infrared Spectroscopy.”, *Journal of Polymer Science Part A: Polymer Chemistry*, Vol. 42, pp. 6283–6298, 2004.

7. Shin, J., H. Matsushima, J.W. Chan, and C.E. Hoyle, “Segmented Polythiourethane Elastomers Through Sequential Thiol-ene And Thiol-isocyanate Reactions.”, *Macromolecules*, Vol. 42, pp. 3294–3301, 2009.

8. Hoyle, C.E., T.Y. Lee, and T. Roper, “Thiol-enes: Chemistry Of The Past With Promise For The Future.”, *Journal of Polymer Science, Part A: Polymer Chemistry*, Vol. 42, pp. 5301–5338, 2004.

9. Li, Q., H. Zhou, D.A. Wicks, and C.E. Hoyle, “Thiourethane-based Thiol-ene HighTg Networks: Preparation, Thermal, Mechanical, And Physical Properties.”, *Journal of Polymer Science Part A: Polymer Chemistry*, Vol. 45, pp. 5103–5111, 2007.

10. Roper, T.M., C.A. Guymon, E.S. Jonsson, and C.E. Hoyle, “Influence Of The Alkene Structure On The Mechanism And Kinetics Of Thiol-alkene Photopolymerizations With Real-time Infrared Spectroscopy.”, *Journal of Polymer Science Part A: Polymer Chemistry*, Vol. 42, pp. 6283–6298, 2004.

11. Khire, V.S., D.S.W. Benoit, K.S. Anseth, and C.N. Bowman, “Ultrathin Gradient Films Using Thiol-ene Polymerizations.”, *Journal of Polymer Science, Part A: Polymer Chemistry*, Vol. 44, pp. 7027–7039, 2006.

12. Cramer, N.B., S.K. Reddy, A.K. O’Brien, and C.N. Bowman, “Thiol - Ene Photopolymerization Mechanism And Rate Limiting Step Changes For Various Vinyl Functional Group Chemistries.”, *Macromolecules*, Vol. 36, pp. 7964–7969, 2003.

13. Carioscia, J.A., J.W. Stansbury, and C.N. Bowman, “Evaluation And Control Of Thiol-ene/thiol-epoxy Hybrid Networks.”, *Polymer*, Vol. 48, pp. 1526–1532, 2007.

14. Reddy, S.K., N.B. Cramer, and C.N. Bowman, “Thiol-vinyl Mechanisms. 1. Termination And Propagation Kinetics In Thiol-ene Photopolymerizations.”, *Macromolecules*, Vol. 39, pp. 3673–3680, 2006.

15. Okay, O., and C.N. Bowman, “Kinetic Modeling Of Thiol-ene Reactions With Both Step And Chain Growth Aspects.”, *Macromolecular Theory and Simulations*, Vol. 14, pp. 267–277, 2005.

16. Cramer, N.B., T. Davies, A.K. O’Brien, and C.N. Bowman, “Mechanism And Modeling Of A Thiol-ene Photopolymerization.”, *Macromolecules*, Vol. 36, pp. 4631–4636, 2003.

17. Khire, V.S., Y. Yi, N.A. Clark, and C.N. Bowman, “Formation And Surface Modification Of Nanopatterned Thiol-ene Substrates Using Step And Flash Imprint Lithography.”, *Advanced Materials*, Vol. 20, pp. 3308–3313, 2008.

18. Reddy, S.K., N.B. Cramer, and C.N. Bowman, “Thiol-vinyl Mechanisms. 2. Kinetic Modeling Of Ternary Thiol-vinyl Photopolymerizations.”, *Macromolecules*, Vol. 39, pp. 3681–3687, 2006.

19. Carlmark, A., C. Hawker, A. Hult, and M. Malkoch, “New Methodologies In The Construction Of Dendritic Materials.”, *Chem. Soc. Rev.*, Vol. 38, pp. 352–362, 2009.

20. DeForest, C.A., B.D. Polizzotti, and K.S. Anseth, “Sequential Click Reactions For Synthesizing And Patterning Three-dimensional Cell Microenvironments.”, *Nature Materials*, Vol. 8, pp. 659–664, 2009.

21. Jonkheijm, P., D. Weinrich, M. Köhn, H. Engelkamp, P.C.M. Christianen, J. Kuhlmann, J.C. Maan, D. Nüsse, H. Schroeder, R. Wacker, R. Breinbauer, C.M. Niemeyer, and H. Waldmann, “Photochemical Surface Patterning By The Thiol-ene Reaction.”, *Angewandte Chemie - International Edition*, Vol. 47, pp. 4421–4424, 2008.

22. Chen, G., S. Amajjahe, and M.H. Stenzel, “Synthesis Of Thiol-linked Neoglycopolymers And Thermo-responsive Glycomicelles As Potential Drug Carrier.”, *Chemical Communications*, Vol. 124, pp. 1198, 2009.

23. Natarajan, L. V., C.K. Shepherd, D.M. Brandelik, R.L. Sutherland, S. Chandra, V.P. Tondiglia, D. Tomlin, and T.J. Bunning, “Switchable Holographic Polymer-dispersed Liquid Crystal Reflection Gratings Based On Thiol-ene Photopolymerization.”, *Chemistry of Materials*, Vol. 15, pp. 2477–2484, 2003.

24. Northrop, B.H., and R.N. Coffey, “Thiol–Ene Click Chemistry: Computational And Kinetic Analysis Of The Influence Of Alkene Functionality.”, *Journal of the American Chemical Society*, Vol. 134, pp. 13804–13817, 2012.

25. Ito, O., and M. Matsuda, “Reactivities Of Cycloalkenes Toward Phenylthio Radicals.”, *The Journal of Organic Chemistry*, Vol. 49, pp. 17–20, 1984.

26. Morgan, C.R., F. Magnotta, and A.D. Ketley, “Thiol/ene Photocurable Polymers.”, *Journal of Polymer Science: Polymer Chemistry Edition*, Vol. 15, pp. 627–645, 1977.

27. Ito, O., and M. Matsuda, “New Dual Parameters For Radical Reactivities Of Vinyl Monomers.”, *Progress in Polymer Science*, Vol. 17, pp. 827–874, 1992.

28. Fischer, H., and L. Radom, “Factors Controlling The Addition Of Carbon-Centered Radicals To Alkenes-An Experimental And Theoretical Perspective.”, *Angewandte Chemie (International ed. in English)*, Vol. 40, pp. 1340–1371, 2001.

29. Degirmenci, I., and M.L. Coote, “Comparison Of Thiyl, Alkoxyl, And Alkyl Radical Addition To Double Bonds: The Unusual Contrasting Behavior Of Sulfur And Oxygen Radical Chemistry.”, *The Journal of Physical Chemistry A*, Vol. 120, pp. 1750–1755, 2016.

30. Degirmenci, I., T.F. Ozaltin, O. Karahan, V. Van Speybroeck, M. Waroquier, and V. Aviyente, “Origins Of The Solvent Effect On The Propagation Kinetics Of Acrylic Acid And Methacrylic Acid.”, *Journal of Polymer Science, Part A: Polymer Chemistry*, Vol. 51, pp. 2024–2034, 2013.

31. Walling, C., and W. Helmreich, “Reactivity And Reversibility In The Reaction Of Thiyl Radicals With Olefins.”, *Journal of the American Chemical Society*, Vol. 81, pp. 1144–1148, 1959.

32. T. M. Roper, C. E. Hoyle, D.H.M., “Reaction Enthalpies Of Monomers Involved In Photopolymerization.”, *Photo-chemistry and UV Curing*, pp. 253 – 264, 2006.

33. Jacobine, A. F. Fouassier, J. D.; Rabek, J. F., E., “In Radiation Curing In Polymer Science And Technology III.”, *In Radiation Curing in Polymer Science and Technology III*, pp. 219–268, 1993.

34. Mayo, F.R., and C. Walling, “The Peroxide Effect In The Addition Of Reagents To Unsaturated Compounds And In Rearrangement Reactions.”, *Chemical Reviews*, Vol. 27, pp. 351–412, 1940.

35. Cristol, S.J., and G.D. Brindell, “Additions To Bicyclic Olefins. P-Thiocresol And Norbornylene.”, *Journal of the American Chemical Society*, Vol. 76, pp. 5699–5703, 1954.

36. Litwinienko, G., A.L.J. Beckwith, and K.U. Ingold, “The Frequently Overlooked Importance Of Solvent In Free Radical Syntheses.”, *Chemical Society Reviews*, Vol. 40, pp. 2157, 2011.

37. Litwinienko, G., and K.U. Ingold, “Solvent Effects On The Rates And Mechanisms Of Reaction Of Phenols With Free Radicals.”, *Accounts of Chemical Research*, Vol. 40, pp. 222–230, 2007.

38. Abboud, J.L.M., C. Roussel, E. Gentric, J. Lauransan, K. Sraidi, G. Guihéneuf, M.J. Kamlet, and R.W. Taft, “Studies On Amphiprotic Compounds. 3. Hydrogen-Bonding Basicity Of Oxygen And Sulfur Compounds.”, *Journal of Organic Chemistry*, Vol. 53, pp. 1545–1550, 1988.

39. Tronche, C., F.N. Martinez, J.H. Horner, M. Newcomb, M. Senn, and B. Giese, “Polar Substituent And Solvent Effects On The Kinetics Of Radical Reactions With Thiols.”, *Tetrahedron Letters*, Vol. 37, pp. 5845–5848, 1996.

40. Parr, R.G., and Y. Weitao, “Density-Functional Theory of Atoms and Molecules.”, *ebrary e-Book Collection* 1994.

41. Becke, A.D., “A New Mixing Of Hartree–Fock And Local Density-functional Theories.”, *The Journal of Chemical Physics*, Vol. 98, pp. 1372, 1993.

42. Becke, A.D., “Density-functional Exchange-energy Approximation With Correct Asymptotic Behavior.”, *Physical Review A*, Vol. 38, pp. 3098–3100, 1988.

43. Roos, B.O., ed., “Lecture Notes in Quantum Chemistry II.”, *Springer-Verlag*, Vol. 64 1994.

44. Leach, A.R., “Molecular Modelling. Principles And Applications.”, pp. 262–269, 2001.

45. Lee, C., W. Yang, and R.G. Parr, “Development Of The Colle-Salvetti Correlation-energy Formula Into A Functional Of The Electron Density.”, *Physical Review B*, Vol. 37, pp. 785–789, 1988.

46. Becke, A.D., “Density-functional Thermochemistry. III. The Role Of Exact Exchange.”, *The Journal of Chemical Physics*, Vol. 98, pp. 5648–5652, 1993.

47. Pauling, L., “The nature of the chemical bond. iv. the energy of single bonds and the relative electronegativity of atoms.”, *Journal of the American Chemical Society*, Vol. 54, pp. 3570–3582, 1932.

48. Tapia, O., B.J., “Solvent Effects And Chemical Reactivity.”, *Kluwer Academic Publishers*, Vol. 17, 1984.

49. Cramer, C.J., and D.G. Truhlar, “Implicit Solvation Models: Equilibria, Structure, Spectra, And Dynamics.”, *Chemical Reviews*, Vol. 99, pp. 2161–2200, 1999.

50. Barone, V., M. Cossi, and J. Tomasi, “Geometry Optimization Of Molecular Structures In Solution By The Polarizable Continuum Model.”, *Journal of Computational Chemistry*, Vol. 19, pp. 404–417, 1998.

51. Barone, V., and M. Cossi, “Quantum Calculation Of Molecular Energies And Energy Gradients In Solution By A Conductor Solvent Model.”, *The Journal of Physical Chemistry A*, Vol. 102, pp. 1995–2001, 1998.

52. M.J. Frisch, G.W. Trucks, H.B. Schlegel, G.E. Scuseria, M.A. Robb, J.R.C., M.C. G. Scalmani, J. Cioslowski, “Gaussian 09 Revision E.01, Gaussian Inc. Wallingford CT.”, *Gaussian 09 Revision E.01* 2010.

53. Neves, R.P.P., P.A. Fernandes, J.C. Varandas, and M.J. Ramos, “Benchmarking Of Density Functionals For The Accurate Description Of Thiol − Disulfide Exchange.”, *J. Chem. Theory Comput.*, Vol. 10, pp. 4842–4856, 2014.

54. Griller, D., and K.U. Ingold, “Persistent Carbon-centered Radicals.”, *Accounts of Chemical Research*, Vol. 9, pp. 13–19, 1976.

55. Matsunaga, N., D.W. Rogers, and A.A. Zavitsas, “Pauling’s Electronegativity Equation And A New Corollary Accurately Predict Bond Dissociation Enthalpies And Enhance Current Understanding Of The Nature Of The Chemical Bond.”, *Journal of Organic Chemistry*, Vol. 68, pp. 3158–3172, 2003.

56. Coote, M.L., C.Y. Lin, and A.A. Zavitsas, “Inherent And Transferable Stabilization Energies Of Carbon- And Heteroatom-centred Radicals On The Same Relative Scale And Their Applications.”, *Physical chemistry chemical physics : PCCP*, Vol. 16, pp. 8686–96, 2014.

57. Dénès, F., M. Pichowicz, G. Povie, and P. Renaud, “Thiyl Radicals In Organic Synthesis.”, *Chemical Reviews*, Vol. 114, pp. 2587–2693, 2014.

58. Bordwell, F.G., X.-M. Zhang, A. V. Satish, and J.-P. Cheng, “Assessment Of The Importance Of Changes In Ground-State Energies On The Bond Dissociation Enthalpies Of The O-H Bonds In Phenols And The S-H Bonds In Thiophenols.”, *Journal of the American Chemical Society*, Vol. 116, pp. 6605–6610, 1994.

59. Bordwell, F.G., X.M. Zhang, A. V. Satish, and J.P. Cheng, “Assessment Of The Importance Of Changes In Ground-State Energies On The Bond Dissociation Enthalpies Of The O-H Bonds In Phenols And The S-H Bonds In Thiophenols.”, *Journal of the American Chemical Society*, Vol. 116, pp. 6605–6610, 1994.

60. Skinner, E.K., F.M. Whiffin, and G.J. Price, “Room Temperature Sonochemical Initiation Of Thiol-ene Reactions.”, *Chemical Communications*, Vol. 48, pp. 6800, 2012.

61. Campos, L.M., K.L. Killops, R. Sakai, J.M.J. Paulusse, D. Damiron, E. Drockenmuller, B.W. Messmore, and C.J. Hawker, “Development Of Thermal And Photochemical Strategies For Thiol-ene Click Polymer Functionalization.”, *Macromolecules*, Vol. 41, pp. 7063–7070, 2008.

62. Dondoni, A., “The Emergence Of Thiol-ene Coupling As A Click Process For Materials And Bioorganic Chemistry.”, *Angewandte Chemie - International Edition*, Vol. 47, pp. 8995–8997, 2008.

63. Degirmenci, I., and M.L. Coote, “Effect Of Substituents On The Stability Of Sulfur-Centered Radicals.”, *Journal of Physical Chemistry A*, Vol. 120, pp. 7398–7403, 2016.

64. Tedder, J.M., “Which Factors Determine The Reactivity And Regioselectivity Of Free Radical Substitution And Addition Reactions?”, *Angewandte Chemie International Edition in English*, Vol. 21, pp. 401–410, 1982.

65. Lalevée, J., X. Allonas, and J.P. Fouassier, “Addition Of Carbon-centered Radicals To Double Bonds: Influence Of The Alkene Structure.”, *Journal of Organic Chemistry*, Vol. 70, pp. 814–819, 2005.

66. Moscatelli, D., M. Dossi, C. Cavallotti, and G. Storti, “Density Functional Theory Study Of Addition Reactions Of Carbon-centered Radicals To Alkenes.”, *Journal of Physical Chemistry A*, Vol. 115, pp. 52–62, 2011.

67. Hammond, G.S., “A Correlation Of Reaction Rates.”, *Journal of the American Chemical Society*, Vol. 77, pp. 334–338, 1955.

68. Evans, M.G., and M. Polanyi, “Inertia And Driving Force Of Chemical Reactions.”, *Transactions of the Faraday Society*, Vol. 34, pp. 11, 1938.

69. Coote, M.L., C.Y. Lin, A.L.J. Beckwith, and A.A. Zavitsas, “A Comparison Of Methods For Measuring Relative Radical Stabilities Of Carbon-centred Radicals.”, *Physical Chemistry Chemical Physics*, Vol. 12, pp. 9597, 2010.

70. Hioe, J., H. Zipse, P.E.M. Siegbahn, G. Bar, J. Robblee, S. Kacprzak, M. Kaupp, R.G. Griffin, M. Bennati, J. Stubbe, J. Stubbe, and N. Lees, “Radical Stability And Its Role In Synthesis And Catalysis.”, *Organic & Biomolecular Chemistry*, Vol. 8, pp. 3609, 2010.

71. Griesbaum, K., “Problems And Possibilities Of The Free Radical Addition Of Thiols To Unsaturated Compounds.”, *Angewandte Chemie International Edition in English*, Vol. 9, pp. 273–287, 1970.

72. Sivertz, C., W. Andrews, W. Elsdon, and K. Graham, “Mechanism Of Free Radical Attack On Double Bonds.”, *Journal of Polymer Science*, Vol. 19, pp. 587–588, 1956.

73. Sivertz, C., “Studies Of The Photoinitiated Addition Of Mercaptans To Olefins. IV. General Comments On The Kinetics Of Mercaptan Addition Reactions To Olefins Including Cis-trans Forms.”, *The Journal of Physical Chemistry*, Vol. 63, pp. 34–38, 1959.

74. Graham, D.M., R.L. Mieville, R.H. Pallen, and C. Sivertz, “Photo-initiated reactions of thiols and olefins: ii. the addition of methanethiol to unconjugated olefins.”, *Canadian Journal of Chemistry*, Vol. 42, pp. 2250–2255, 1964.

75. Ito, O., and M. Matsuda, “Evaluation Of Addition Rates Of Thiyl Radicals To Vinyl Monomers By Flash Photolysis. 5. Polar Effects In Addition Reactions Of Benzenethiyl Radicals To Substituted Styrenes And .alpha.-methylstyrenes Determined By Flash Photolysis.”, *Journal of the American Chemical Society*, Vol. 104, pp. 1701–1703, 1982.

76. Osamu, I., and M. Minoru, “Evaluation Of Addition Rates Of The Thiyl Radicals To Vinyl Monomers By Flash Photolysis. 2.1 Substituent Effect On Addition Of Substituted Benzenethiyl Radicals To Methyl Methacrylate Or Styrene.”, *Journal of the American Chemical Society*, Vol. 101, pp. 5732–5735, 1979.

77. Ito, O., and M. Matsuda, “Evaluation Of Addition Rates Of P-Chlorobenzenethiyl Radical To Vinyl Monomers By Means Of Flash Photolysis.”, *Journal of the American Chemical Society*, Vol. 101, pp. 1815–1819, 1979.

78. Sato, T., M. Abe, and T. Otsu, “Application Of Spin Trapping Technique To Radical Polymerization, 16. Photo-decomposition Of Diphenyl Disulfide And Initiation Mechanism: Evaluation Of Relative Reactivities Of Vinyl Monomers Toward Phenylthio Radical.”, *Die Makromolekulare Chemie*, Vol. 180, pp. 1165–1174, 1979.

79. Schoneich, C., K.-D. Asmus, and M. Bonifacic, “Determination Of Absolute Rate Constants For The Reversible Hydrogen-atom Transfer Between Thiyl Radicals And Alcohols Or Ethers.”, *Journal of the Chemical Society, Faraday Transactions*, Vol. 91, pp. 1923, 1995.

80. Newcomb, M., A.G. Glenn, and M.B. Manek, “Rate Constants And Arrhenius Functions For Hydrogen Atom Transfer From Tert-Butyl Thiol To Primary Alkyl Radicals.”, *Journal of Organic Chemistry*, Vol. 54, pp. 4603–4606, 1989.

81. Pogocki, D., and C. Schöneich, “Thiyl Radicals Abstract Hydrogen Atoms From Carbohydrates: Reactivity And Selectivity.”, *Free Radical Biology and Medicine*, Vol. 31, pp. 98–107, 2001.

82. Nauser, T., W.H. Koppenol, and C. Schoöneich, “Reversible Hydrogen Transfer Reactions In Thiyl Radicals From Cysteine And Related Molecules: Absolute Kinetics And Equilibrium Constants Determined By Pulse Radiolysis.”, *Journal of Physical Chemistry B*, Vol. 116, pp. 5329–5341, 2012.